Resource-constrained Avionics Design for CubeSats

James "Mic" Byrne, Prof. Kerri Cahoy

Resource-constrained Avionics Design for CubeSats

James "Mic" Byrne, Prof. Kerri Cahoy

<Month Year>   SSL # <02-16>

Resource-constrained Avionics Design for CubeSats

by

James Michael Byrne, Jr

Abstract

We present an optimization approach to CubeSat avionics design which considers the consumption of some resources (electrical power, volume) and production of others (processing power, volatile memory, non-volatile memory, and radiation tolerance) in a quantitative optimization analysis.

We present the avionics hardware design for the Microwave Radiometer Technology Acceleration (MiRaTA) 3U CubeSat, funded by the NASA Earth Science Technology Office (ESTO), as a case study for our optimization analysis. MiRaTA will demonstrate a three-band microwave radiometer and GPS radio occultation (GPSRO) sensor suite for profiling atmospheric temperature, humidity, and cloud ice. The goal is to increase the Technology Readiness Level (TRL) of the weather-sensing technology from TRL 5 to TRL 7[1].

The avionics system is the "central nervous system" of the spacecraft, managing interfaces with every subsystem and between the Bus and Payload. MiRaTA's avionics design supports the Payload, which is tasked with the science mission to gather and process appropriate radiometer and GPSRO data, and the Bus, which comprises subsystems to handle attitude determination and control (ADC), power regulation and distribution, communications with the ground station, thermal management, and a suite of sensors and telemetry components. MiRaTA's avionics system uses a custom designed motherboard with a PIC24FJ256GB210 microcontroller to command activity in the Bus and manage data and power for the Payload. This custom Motherboard – dubbed the "Micron Motherboard" – leverages many of the advantages of the popular Pumpkin Motherboard but with reduced complexity and improved performance. The MiRaTA avionics system is also designed to minimize the number and length of cables, simplify connector uniformity, and improve accessibility. The design improvement in avionics hardware from MicroMAS to MiRaTA is quantified using an optimization coefficient: 1.522. We expect optimization coefficients to range typically from -4 to +4, so this design indicates a modest improvement.

---

[1] http://esto.nasa.gov/files/trl_definitions.pdf

Although the avionics for MiRaTA are based on a previous mission, the Micro-sized Microwave Atmospheric Satellite (MicroMAS), in order to accommodate the tri-band radiometer hardware, the GPSRO experiment, and a backup radio, the available volume for MiRaTA has been significantly reduced compared to MicroMAS. Additionally, a shorter time from conception to launch, higher-altitude orbit, and increased power requirements have called for optimization of existing avionics design as well as new design elements. The challenge for MiRaTA is to maintain and improve functionality while balancing size, weight, cost, time, and power without sacrificing functionality in the harsh environmental conditions of space.

Thesis Supervisor: Kerri Cahoy
Title: Assistant Professor of Aeronautics of Astronautics

Acknowledgments

Table of Contents

List of Figures

List of Tables

Key Nomenclature

MiRaTA	Microwave Radiator Technology Acceleration (spacecraft)
MicroMAS	Micro-sized Microwave Atmospheric Satellite
COTS	Commercial-off-the-shelf
SWaP	Size, Weight, and Power
IMA	Integrated Modular Avionics
EPS	Electrical Power System
PDU	Power Distribution Unit
NASA	National Aeronautics and Space Administration
GPS	Global Positioning System
TRL	Technology Readiness Level
COTS	Commercial Off-The-Shelf
ADCS	Attitude Determination and Control Systems
RCS	Reaction Control System
TTL	Transistor-transistor Logic
CMOS	Complimentary Metal-Oxide Semiconductor
MEMS	Micro Electro-Mechanical Systems
CPU	Central Processing Unit
FPGA	Field Programmable Gate Array
SWaP	Size, Weight, and Power
EPS	Electrical Power System
PDU	Power Distribution Unit
IMA	Integrated Modular Avionics
I^2C	Inter-Integrated Circuits
UART	Universal Asynchronous Receive/Transmit
SPI	Serial Peripheral Interface
MOSI	Master Output / Slave Input
MISO	Master Input / Slave Output
SCK	Signal Clock
SS	Slave Select
GPIO	General Purpose Input/Output
kB	Kilobyte
MB	Megabyte
GB	Gigabyte
ESTO	Earth Science Technology Office
MIT	Massachusetts Institute of Technology
GPSRO	GPS Radio Occultation
TRL	Technology Readiness Level
LVLH	Local-Vertical Local-Horizontal
AIC	Algorithmic Information Content
PIM	Payload Interface Module
PPOD	Poly Picosatellite Orbital Deployer
LEO	Low-Earth Orbit

MIPS	Million Instructions Per Second
TID	Total Ionizing Dose
PPM	Pluggable Processor Module
ROM	Read-Only Memory
RF	Radio Frequency
LST	Low-Speed Transmitter
SPDT	Single-Pole Double-Throw
LNA	Low Noise Amplifier
UHF	Ultra High Frequency
BIB	Bottom Interface Board
IMU	Inertial Measurement Unit
CSS	Coarse Sun Sensor
RTD	Resistance Temperature Detector
TKD	Thermal Knife Driver
TIB	Top Interface Board
USB	Universal Serial Bus
RAM	Random Access Memory
RRAM	Resistive Random Access Memory
FRAM	Ferro-electric Random Access Memory
SPST	Single-Pole Single-Throw
CPI	Cycles Per Instruction
ESD	Electrostatic Discharge

1   Introduction

1.1 Introduction

The purpose of this thesis is to design an avionics system that maintains or increases functionality (processing power, volatile and non-volatile memory, radiation tolerance) while quantifiably reducing resource consumption (such as volume and electric power). This chapter describes CubeSat avionics, reviewing the environmental and systematic constraints placed on the avionics design, and familiarizing the reader with the MiRaTA spacecraft in order to provide a better context from which to understand the rest of the paper.

1.2 Motivation

1.2.1 Why CubeSats?

Small satellites, which include CubeSats, have seen a rapid rise in popularity. Indeed, Figure 1 displays the dramatic increase in CubeSats launched in just the past three years increasing by almost 450% from 2012 to 2014, from 30 to 130 satellites. However, despite this rapid growth and sizeable number of satellites currently on orbit, the estimated combined cost of every small satellite launched since 2005 remains less than $100 million. (The Tauri Group, 2015) With such a rapid increase in both launched CubeSats as well as individuals, universities, governments, and corporations investing in them, a design optimization analysis should prove beneficial.

Figure 1: Number of CubeSats Launched by Year (2005-2014) (The Tauri Group, 2015)

The introduction of CubeSats, with their small form factor providing low-cost access to space, has sufficiently lowered the barrier to entry into the aerospace industry that dozens of new companies as well as new divisions of existing aerospace firms have sprung up to get in the game. One of the new companies to emerge in the past 15 years is Pumpkin Inc. Pumpkin's founder Andrew Kalman was among the first to recognize the potential for commercialization of CubeSat components, including avionics. Now over a decade since the first version was released, the Pumpkin Motherboard has become something of a staple for a number of small satellites and provides a useful standard from which to approach an optimization of CubeSat avionics. (Pumpkin Inc, 2003)

Once its cost-effectiveness was proven, the CubeSat industry gave rise to companies not centered around just manufacture and sale of components, but driven by the sale of science and data output from the CubeSats themselves. One example of such an up-and-coming company is Planet Labs (formerly Cosmogia Inc). Founded in 2010, Planet Labs set out to utilize an inexpensive CubeSat platform to gather near-real-time images of the Earth's surface for use in agriculture, prospecting, environmental protection, etc. Their efforts have been recognized for pushing the envelope of speed and cost in what they have deemed "agile aerospace." Planet Labs' dedication to shorter and shorter turnaround times from conception to launch, reduced cost without

16

sacrificing robustness, and balance of custom and commercial-of-the-shelf (COTS) components has provided additional inspiration to this author in pushing the envelopes of optimization. (Planet Labs Inc, 2015)

1.2.2 Why Avionics?

Avionics holds a unique role among spacecraft subsystems. Other subsystems such as attitude determination and control systems (ADCS), power, communications, and propulsion must undergo a rigorous trade-space with one another, vying for resources like size, weight, power, and cost. One may have to decide between a larger patch antenna and more body-mounted solar cells, or between reaction wheels and reaction control system (RCS) thrusters. In optimization decisions between subsystems, there is always a give and a take. With avionics, it seems, there is only take. There is only one direction for avionics optimization in each of these spaces: it is to be as small, light, cheap, and power-starved as possible, ready as quickly as possible, with improved functionality. This singular directionality of resources makes avionics a relatively straightforward system for optimization.

There are, however, some additional factors which complicate an otherwise straightforward problem. Some more difficult-to-quantify resources such as complexity and risk turn a straightforward optimization equation into a challengingly qualitative assessment. The result of this combination of quantitative (i.e. size and power) and qualitative (i.e. risk and complexity) yields an *approach* rather than a single equation. The purpose of this thesis is to present this approach, supported by numerical assessment where possible.

1.3 Brief History of Satellite Avionics

The remarkable improvements in electronics and software technology over the past half century have contributed significantly to this discussion. The successful launch of the world's first manmade satellite in October of 1957, Sputnik I, began a competition for space dominance between the United States and Russia known as the "space race." (Garber, 2007) With this race for dominance came the need for improved technology. 1958 marked the beginning of a parallel "electronics race" with the invention of the first integrated circuit out of Texas Instruments. (ScienCentral, Inc and the American Institute of Physics, 1999) Soon thereafter came the invention

of transistor-transistor logic (TTL) and complimentary metal-oxide semiconductor (CMOS) technology, which changed the way these integrated circuits communicated with one-another. Micro electro-mechanical systems (MEMS) technology soon followed with Harvey C. Nathanson's Resonant Gate Transistor, which changed the way electronics interacted with the physical world. (United States Patent No. 7102472, 2006) A major leap forward came in 1970 when Intel introduced the first microprocessor , giving not just spacecraft but computers, appliances, and automobiles a means of processing information and, perhaps most importantly, programmability. The introduction of X-ray lithography in 1987 further miniaturized integrated circuits and added credibility to the law proposed by Gordon E. Moore: that the number of transistors able to fit onto a microchip would roughly double each year.

The evolution of capability of consumer electronics is also driving the capabilities of small satellites. The frequent adoption of COTS components on CubeSats means that the microcontrollers that make laptops thinner and smart phones smarter are doing the same for satellite design. In fact, a move toward commercial off-the-shelf components – purchasing entire sensor, computation, and actuation suites from third party vendors – seems to be where the small satellite community seems to be headed. In a recent lecture at the Small Satellite Conference in Logan, Utah, the tradeoffs between COTS and custom components were discussed, as well as methodologies for making decisions on which to use. One presenter, Doug Sinclair, addressed this trend, concluding that "opting for custom [components] can effectively remedy deficiencies in performance but often at the expense of technical and budgetary risks." (2015) Many COTS components, while they are convenient and save development time and monetary cost, can create problems as well by their lack of optimization to the particular mission or task at hand.

1.4 Avionics as a Subsystem

1.4.1 The Avionics Philosophy

If one were to liken a spacecraft to a living organism, the avionics subsystem represents the central nervous system. At its core lies the "brain," that is, the central processing unit (CPU) of the spacecraft. This CPU can be a microcontroller, Field Programmable Gate Array (FPGA), or more complex structure which provides the task management, arithmetic, and signaling that controls all other peripheral components in the avionics system. Similarly, the CPU also interprets

signals coming in from its peripherals and makes decisions either autonomously or from commands sent from a ground station. Much like the way the brain commands the internal organs via the autonomic nervous system to operate without conscious thought, the CPU maintains spacecraft vital system functionality (such as voltage regulation, watchdog timers, and waste management) through pre-determined, hard coded software that operates independent of commands from the ground. Additionally, a suite of sensors normally present on spacecraft including CubeSats, sends information back to the CPU along pre-determined input/output pins akin to the five senses we use to comprehend our environment sending signals along designated neural networks. Understanding this special role of the avionics system as the central nervous system of the spacecraft is essential to understanding its design. (Wang, Wang, Zhou, & Zhai, 2009)

One may point out that a central nervous system on its own, while perhaps "alive," is utterly useless without external organs for mobility, sensing, etc. Indeed, the purpose of an avionics package is not self-evident, but comprehensible only in the presence of the rest of the spacecraft. When one further considers the purpose of a satellite – be it data collection or data distribution – one can quickly conclude that the avionics system must consider the needs of other systems as higher than its own, minimizing its resource utilization while maximizing its functionality. This one-sided interdependence of all other systems of the spacecraft on the avionics system gives rise to an essential element of avionics design: a service-oriented mindset.

Part of service is sacrifice, and sacrifice in space systems invariably involves size, weight, and power (SWaP). Fortunately, with avionics, the question of direction – to conserve or to spend – these vital resources is pre-determined: smaller, lighter, lower power. The optimization of SWaP for avionics, instead of a standard tradeoff, then becomes a simple search for the minimum operational limits which would allow the spacecraft to function, adding some margin, and maximizing functionality given those constraints.

1.4.2 Power Management and Distribution

One way to approach CubeSat avionics design is to break down its responsibilities into two subsections: power management and data management.

A CubeSat, or any spacecraft for that matter, ordinarily has a dedicated power subsystem which regulates voltage, limits current, and provides any number of fault protections against over-voltage, over-current, under-voltage, and under-current (among other) conditions. The nature of a CubeSat (small volume), however, dictates that the power system have a special and integrated relationship with the avionics system. (Obland, et al., 2002)
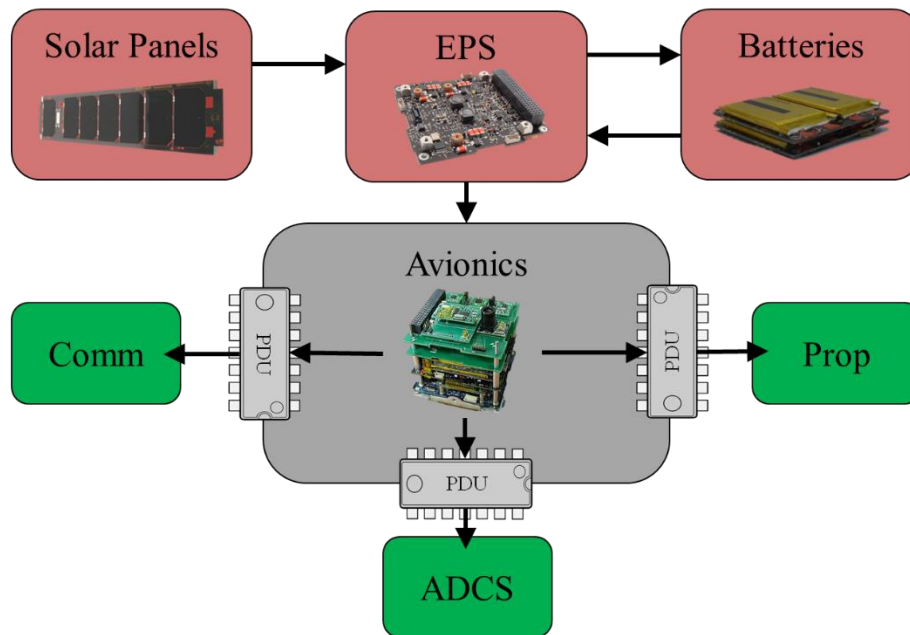
Figure 2: Flow of Power.[2] Power system is shown in red, avionics system in gray, other systems in green. Payload is not included but may be present on some spacecraft with a distinct payload section.

Figure 2 displays the flow of electrons from the power system to the avionics system and on to the remaining power-dependent systems that comprise the spacecraft.[3] Solar panels provide the typical means of acquiring power on orbit available to CubeSats (radioactive isotopes for thermoelectric generators are not yet rated for CubeSats, and some CubeSats have flown short missions with only primary batteries). These solar panels, when exposed to solar radiation, transmit energy to the Electrical Power System (EPS) which in turn regulates the energy to voltage levels and current limits that the rest of the spacecraft will utilize for operation. Any additional

---

[2] Solar panels, EPS, and Batteries courtesy Clyde Space Inc. Avionics image retrieved from https://directory.eoportal.org/documents/163813/197313/ITUpSat1_Auto2

[3] The structure system does not require power and the thermal system was not included.

energy not routed directly to the rest of the spacecraft is used to charge the batteries for use in eclipse or when solar power alone is insufficient for operation.

Once power reaches the avionics system, authority over its flow is transferred. CubeSat avionics systems ordinarily utilize Power Distribution Units (PDUs) to, at a minimum, switch power on or off to peripheral devices within the avionics systems or external devices under the jurisdiction of other systems such as communications, propulsion, or ADCS. Some more sophisticated PDUs also limit current, switch off and report a fault when current limit is reached, and regulate voltage locally themselves. PDUs may also be used, in the event of a serious fault, to prevent power flow to a component or system without jeopardizing the remaining functional elements of the spacecraft. In this manner, the avionics system retains control over power cycling and current limiting to all other spacecraft systems.

In addition to power distribution, some commercial off-the-shelf avionics components have voltage regulation circuitry. This circuitry is very useful in ground testing, as it reduces risk when providing unregulated voltage to power the system. However, it's worth considering the benefit of this luxury (power can just as easily be regulated externally in ground testing) when weighed against the loss of valuable real estate in an already volume-constrained environment.

Additionally, avionics power design must take into account the minimization of ground loops and noise caused by power lines in close proximity to data lines. On orbit, there is only a floating ground. With no true ground into which electrons might terminate, relative differences in floating ground voltages may arise on different structures in the spacecraft. This naturally-occurring phenomenon is accelerated by the charging of spacecraft by particles in orbit around the Earth. Relative differences in ground voltages often results in current on the order of several milliamperes flowing from one location on a ground plane to another, which may be sufficient to mimic a low-power signal, interfere with sensitive sensors, or even damage components. Avionics power design, therefore, must seek to eliminate the channels through which these "ground currents" may flow. (Elkman, 1983)

1.4.3 Data Management and Processing

The avionics system on CubeSats serves as both the central router and the central processor. This second role – as the central processor – is special to many small satellites. Indeed, it has even

called for a rethinking of how we approach avionics design. A growing field of engineers in both the aerospace and airline industries have begun adopting what is being called an Integrated Modular Avionics (IMA) approach to design. In large aircraft and spacecraft, classical avionics design takes the form of a federated architecture. Various self-contained units throughout the spacecraft or aircraft are each allotted their own miniature avionics subsystem, which can be as simple as an amplification circuit up to fully-functional power regulation and distribution, a dedicated processor, and backup communications device. These self-contained units were paired with different payload sensors, attitude control, communications arrays, etc and routed back to a central, larger avionics core which managed the semi-autonomous units and organized their data as efficiently as possible. (Mairaj & Tahir, 2014)

While a federated architecture reduces risk in many key areas, such an approach is simply not feasible given the size, weight, and power restrictions inherent to CubeSat avionics design. An IMA approach, on the other hand, features shared computing (a central processor for all peripherals), an I/O resource pool, and shared communications (including any potential backup communications). Instead of multiple, smaller, semiautonomous brains, a design using Integrated Modular Avionics maintains a single CPU and interchangeable "dumb" peripherals which are all commanded and controlled by a central processor. (Watkins & Walter, 2007) What is lost in computational speed (federated architecture is effectively parallel computing) is more than made up for in reduced SWaP, as well as hardware complexity, at the cost of increased software complexity.

It is also essential to consider the role of avionics as the data router. Fortunately, there are a number of means of transporting data supported by even the simplest microcontroller. The first distinction among data routing methods is that between serial and differential signals. Information in the world of electrons can be broken down into a yes/no dichotomy: "is it on?" or "is it off?" The result is a form of communicating/counting known as "binary." These binary signals, represented by 1's and 0's, travel along data lines in two ways. In a serial communication protocol, one device communicates with another by sending a series (hence, serial) of "high" signals (usually 3.3 or 5V) and "low" signals (0V) which represent the 1's and 0's in a binary message. In a differential protocol, the concept is the same but the execution is different. Instead of a single data line carrying a "high" or a "low," a differential signal uses two distinct data lines, each carrying

the opposite voltage level of the other. For example, a 1 is represented by Line A carrying a "high" and Line B carrying a "low" voltage. A 0 is represented by Line A carrying a "low" and Line B carrying a "high." A design which uses a differential signal will have increased resistance to noise (two lines are better than one), but will pay for it in complexity (two lines means two input/output pins used). Fortunately for CubeSats, noise profile is directly proportional to signal wire length and, even in the most inefficiently routed CubeSat, no wire should ever reach the length where noise would become an issue on a simple serial line. This reserves the need for differential signals in special cases where noise profiles are abnormally high or physical connections demand greater durability.[4] (Verle, PIC Microcontrollers, 2008) (Verle, PIC Microcontrollers - Programming in Basic, 2010)

In the serial family of communications, there are three main protocols utilized by microcontrollers and widely applicable to CubeSat avionics: Inter-Integrated circuits (I^2C), Universal Asynchronous Receive/Transmit (UART), and Serial Peripheral Interface (SPI). The simplest of these protocols from a hardware perspective is I^2C. I^2C takes two pins from a supporting microcontroller: one pin for data, and another for a clock. These two pins form a bus that connects a dedicated master device (usually the main avionics microcontroller) to over 100 slave devices (the various peripheral components and systems on a CubeSat). The master device uses the clock signal, shared by all devices in the I^2C network, to maintain synchronization while sending data to specified slaves on the shared data line, addressing slaves individually by calling out their hardware-specific address. A similar process applies to a Serial Peripheral Interface (SPI) network. As with I^2C, a SPI network can support hundreds of slave devices sharing a common bus, albeit with four necessary lines (three if only one slave is connected): Master Output / Slave Input (MOSI), Master Input / Slave Output (MISO), Signal Clock (SCK), and Slave Select (SS). SPI doubles the necessary line count from I^2C by using dedicated lines for input and output to the master device and using an additional line solely for selecting the slave with which the master

---

[4] For example, MicroMAS (Blackwell, et al., MicroMAS: A First Step Towards a Nanosatellite Constellation for Global Storm Observation, 2013) required twelve communication and power lines to be routed across a slip-ring used to rotate 1/3 of the spacecraft

wants to communicate. This increase in hardware complexity can reduce software complexity, and also results in faster communication than an I^2C bus. (Sidwar, 2015)

Universal Asynchronous Receive/Transmit is an older serial communication protocol that is common in CubeSat avionics designs due to its simplicity and broad support. While slower than both I^2C and SPI, UART gets the job done with only two pins. In a more complex arrangement whereby neither device is master over the other, two additional pins can be allotted for a "handshaking" protocol that allows two-way communication. All of these three main communication protocols allow for complex information "packets" to be sent between devices that spell out more than just the 1's and 0's which carry them, much like how a word means more than just a combination of the letters that comprise it. However, not all pins need be a part of a complex communication protocol. Many integrated circuits have simple General Purpose Input/Output (GPIO) pins which can be set either "high" or "low" by a software command. GPIO pins are best utilized when simple information or switching needs to be conveyed, while more complex data is reserved for the three protocols listed earlier. (Sidwar, 2015)

Table 1: Advantages and disadvantages of major serial communications protocols utilized by microcontrollers

Protocol	Advantages	Disadvantages
General Purpose Input/Output (GPIO)	Simple, requires single pin	Slow, clumsy to send complex data
Inter-Integrated Circuit (I^2C)	Can handle complex data, only requires 2 pins, bus sharing	Not good over long distances, slower than SPI
Serial Peripheral Interface (SPI)	Can handle complex data, bus sharing, clear pin mapping	Requires at least 3 pins,
Universal Asynchronous Receive/Transmit (UART)	Widely used, supports hand-shaking, only requires 2 pins	Not good over long distances, slowest protocol

The IMA approach to avionics design, while it reduces overall complexity by reducing the number of distributed microcontrollers, increases local complexity on the remaining central microcontroller. Of particular note is the number and capability of pins present on this microcontroller. Increasing capability calls for increasing pins, which call for more and more crowded and complex integrated circuit packaging and subsequent board layouts to support them. Additionally, all microcontrollers have a limited number of I^2C, SPI, and UART modules these

pins can support. This sets a limit on the number of peripheral components a CubeSat can support without sacrificing the key advantages to an IMA design.

1.4.4 Reprogrammability

Of crucial note for CubeSat avionics design is the incorporation of reprogrammability. Reprogrammability is achieved by a software program called a "bootloader" that runs every time the microcontroller is reset. It waits for a command from the ground station to enter "reprogramming mode." If such a command is received, it stops the standard boot-up operation, enters reprogramming mode, and downloads the code sent from the ground station to replace the existing software without altering the bootloader itself. If a reset microcontroller receives no command from the ground station to reprogram within a certain amount of time after its reset, it assumes no reprogramming is necessary and boots up the existing flight software.

On orbit changes often necessitate, at minimum, updates to software and, at most, complete changes to the operating system. While some satellites do not have the ability to be reprogrammed, for CubeSats this functionality is all but essential. The shorter development time and reduced depth of testing inherent to CubeSat projects increases the likelihood of a software patch or alternation on orbit. This need for reprogrammability brings with it consequences for both hardware and software design in the avionics system. For example, fault tolerance to radiation-induced upsets is essential so as to avoid an unrecoverable error to the bootloader.

Watchdog timers are also important to automatically reset the system in the event that a software update causes an inability to manually reset the system. A watchdog timer is a low-level timer, operating in parallel with the rest of the flight software, counting down from a predetermined value to zero. The watchdog timer must be acknowledged periodically (we say it must be "pet" as one pets a dog) and reset back to its original value. If it is ever not acknowledged in time before countdown reaches zero, it is assumed that a problem has arisen which has prevented the flight software from petting it, and the software is completely reset. This safeguard prevents software-induced errors (such as priority or inheritance-borne deadlock) as well as hardware (radiation-induced) lockups.

Of additional importance, the ability to store a "golden image" of the original flight software in non-volatile memory is beneficial so as to return to a working version in the event that new software is inoperable or flawed.

1.4.5 Standard Avionics Structures

CubeSat avionics typically follow a "stack" design, whereby circuit boards are stacked on top of one another sharing a common header bus. A stack design's strengths are in its simplicity (fewer cables, centralized location), freedom of placement anywhere within a CubeSat structure that is most optimal to minimize routing lengths to other systems, decreased exposure to radiation, and isolation of noise crossing over between analog and digital signals. Crucially, a stack such as that shown in Figure 3 benefits from its compatibility with commercial off-the-shelf components (many share common bus headers), which is perhaps the most compelling reason to choose such a design: freedom of custom/COTS interchangeability.

Figure 3: Example of an avionics "stack"[5]

Although popular, the avionics stack design is not the only means of physically laying out a CubeSat's avionics system. One major disadvantage of the avionics stack is its inefficient use of volume. Given a CubeSat's already volume-starved structure, the large gaps present between

---

[5] Retrieved from http://images.spaceref.com/news/2011/Stack-with-background_300dp.jpg

boards in a stack are very wasteful, even if they are thermally advantageous (large radiation surfaces). One approach to minimize this wasted volume is to place circuit boards around the perimeter of a CubeSat, parallel with or even into its main walls. (Manyak & Bellardo, 2011) While this design certainly saves volume, it pays for it in simplicity, exposure to radiation, and crucially, it requires nearly all its circuitry and structure to be custom designed, as most COTS components are not designed with this strategy in mind. Another design strategy, moving in the opposite direction, is to rely *entirely* on COTS components, which quickly yields a bulkier avionics subsystem attributed to the commercial demand that avionics be applicable to many environments and missions, yielding superfluous components and even entire boards.

1.4.6 State of the Art CubeSat Avionics

The current state of the art of CubeSat avionics is represented by both custom and commercial projects, and many CubeSat avionics systems consist of a combination of custom and COTS. Of the popular COTS components, those manufactured by Pumpkin Inc. are among the most popular. A representative but incomplete subset of avionics manufacturers and information regarding their core COTS avionics capabilities are listed in Table 2.

Table 2: List of several major CubeSat avionics vendors and their core avionics specifications, obtained from open-source company websites. This list is not exhaustive.

Company	Motherboard	Main Processor	Clock Speed (MHz)	Volatile Memory	Non-Volatile Memory	Size
Pumpkin[6] Inc.	Pumpkin	PIC24	8	96 KB	32 MB	9.0 x 9.6cm
Space Micro Inc.[7]	Proton 200K	TI 320C6	200	285 MB	8 GB	10 x 16cm
GomSpace[8]	NanoMind A3200	AVR32	64	32 MB	128 MB	6.5 x 4.0cm
Tyvak[9]	Intrepid	AT91SAM9G20	133	128 MB	544 MB	8.3 x 9.4cm

---

[6] http://www.cubesatkit.com/docs/datasheet/DS_CSK_MB_710-00484-E.pdf

[7] http://www.spacemicro.com/assets/datasheets/digital/slices/proton200k-dsp.pdf

[8] http://www.gomspace.com/documents/gs-ds-nanomind-a3200-1.3.pdf

[9] http://tyvak.com/intrepidsystemboard/

Satellite	Organization	Main Processor	Clock Speed (MHz)	Volatile Memory	Non-Volatile Memory	Operating System
Nano Avionics[10]	SatBus 1C0	ARM Cortex M4	8	192 KB	32 MB	9.0 x 9.6cm

The current state of the art in CubeSat avionics is heavily influenced by these COTS components, but many missions also choose to fly either entirely custom or partially custom avionics systems. Table 3 shows a non-exhaustive list of missions with at least partial custom avionics design.

Table 3: PolySat's comparison of current and recent custom avionics core designs (Manyak & Bellardo, 2011)

Satellite	Organization	Main Processor	Clock Speed (MHz)	Volatile Memory	Non-Volatile Memory	Operating System
PolySat 1	Cal Poly	PIC18F6720	4	3.75 KB	256 KB	Custom
PolySat 2	Cal Poly	AT91SAM9G20	400	64 MB	528 MB	Linux
Cute-1.7+APDII	Tokyo Inst. of Tech.	ARMV4I	400	32 MB	128 MB	Windows CE.NET
MEROPE	Montana State	MC68HC812A4	8	1 kB	154 kB	Custom
QuakeSat	Stanford	ZFx86 486 Clone	100	16 MB	1 MB	Linux
AAUSAT-II	Aalborg University	AT91SAM7A1	40	2 MB	8 MB	Unknown
STUDSAT	India – 7 Universities	AT91SAM91260	180	64 kB	512 kB	VxWorks

It is important to note that Table 2 and Table 3 are non-exhaustive and cover only a few of the many COTS avionics packages and custom missions flown over the years. Ultimately, the current state of CubeSat avionics design comes down to a tradeoff between these COTS and custom components. Although each mission is different and likely calls for different degrees of customization, wherever it is practical, COTS components should be utilized in order to save on both time and cost. In particular, for one-time missions, COTS components, with their lower initial investment in labor and money, make the most sense. Also, the existence of active user communities for many COTS hardware components and their associated drivers and software makes development and debugging significantly easier, as help is more readily available.

---

[10] http://n-avionics.com/flight_computers

Commercial off-the-shelf components come with some significant caveats, however. Because they were not designed with any one particular mission in mind, any CubeSat which uses a COTS avionics board will almost certainly have unused functionality. Additionally, the debugging process for COTS components can be painstaking, as the full extent of software and hardware design is not always shared with the customer. (Krodel, 2001)

Custom avionics serve an important role as well, as many of their strengths play to the weaknesses of COTS components. In particular, custom avionics, when designed correctly, optimize their use of resources for a particular mission and, should that mission repeat or change even slightly, eventually return on their high initial investment. Custom avionics also provide additional design flexibility, enabling designers of CubeSats to adapt more easily to the needs of the mission, and to branch out from the avionics stack design discussed in section 1.4.5 for which most COTS components are designed. Where custom avionics suffer is in utilization of time and money. With a high initial investment, custom avionics are not always the right decision when constrained by these key resources that made the CubeSat platform so appealing in the first place: quick and cheap development. An additional complication comes when attempting to mix COTS and custom components in a disadvantage they both share: some COTS packages are meant to interface only with other COTS components from the same product line, and introducing custom avionics can quickly over-complicate the design. (Wilcock, Totten, Gleave, & Wilson, 2001)

Table 4: Comparison of advantages and disadvantages of COTS and custom avionics

Commercial Off-the-Shelf	Custom
Advantages	
No development time	Adaptable to the mission
Low initial investment	Full resource utilization
User community	Structural flexibility
Disadvantages	
Unused functionality	Higher initial investment
Not designed with the future in mind	Some development time
Difficult debugging	May not interface with COTS devices

The bottom line is that an optimization point between COTS and custom exists for every CubeSat avionics design, and it is worth considering the advantages and disadvantages of each when identifying that optimization point.

1.5 Introduction to MiRaTA

1.5.1 MiRaTA's Precursor: MicroMAS

This thesis will focus on the Microwave Radiometer Technology Acceleration (MiRaTA) spacecraft as a case study for understanding avionics optimization. However, in order to understand MiRaTA, it is worth discussing MiRaTA's precursor mission: the Micro-sized Microwave Atmospheric Satellite (MicroMAS).

MicroMAS is a "dual-spinning 3U CubeSat equipped with a nine-channel passive microwave spectrometer observing near the 118.75-GHz oxygen absorption line." The purpose of this microwave spectrometer, also called a radiometer, is to observe upper-atmospheric microwave emissions in order to make temperature maps which can be used to predict or detect thunderstorms, tropical cyclones, and hurricanes in the lower atmosphere. Orbiting in a local-vertical local-horizontal orientation, assisted by its "space dart" form factor, the 1U payload housing this radiometer rotates approximately once per second, allowing MicroMAS to sweep a large area of atmosphere in its 2.5 degree beamwidth and 20 km diameter footprint and, when pointing into the coldness of space, recalibrate on each pass.
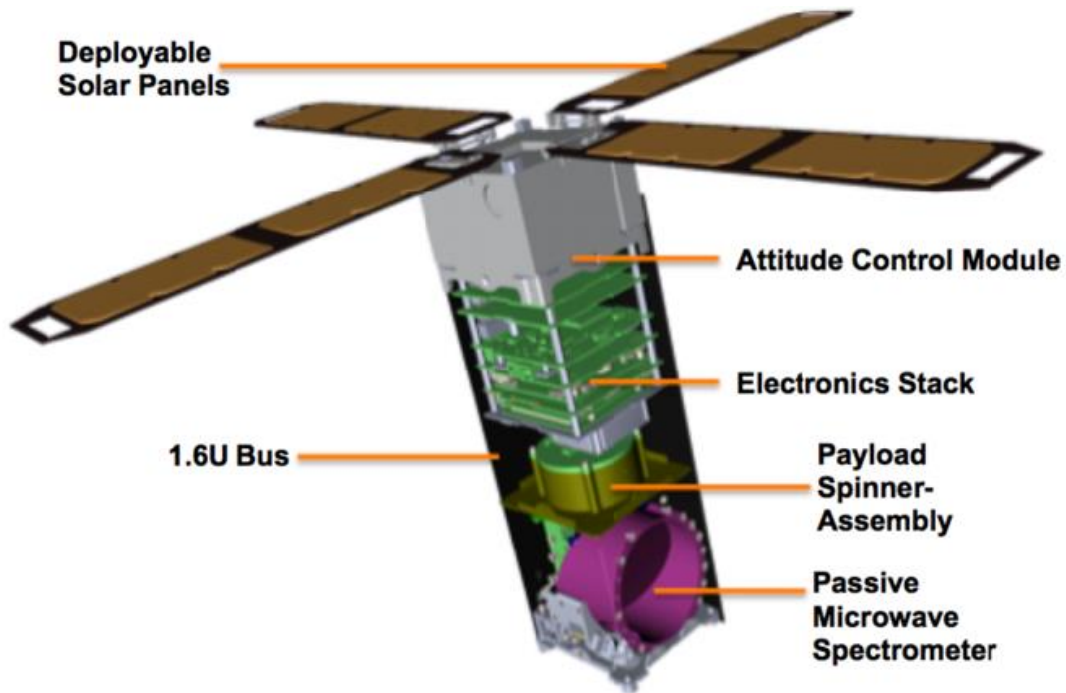
Figure 4: Micro-sized Microwave Atmospheric Satellite (MicroMAS) overall design (Blackwell, et al., MicroMAS: A First Step Towards a Nanosatellite Constellation for Global Storm Observation, 2013)
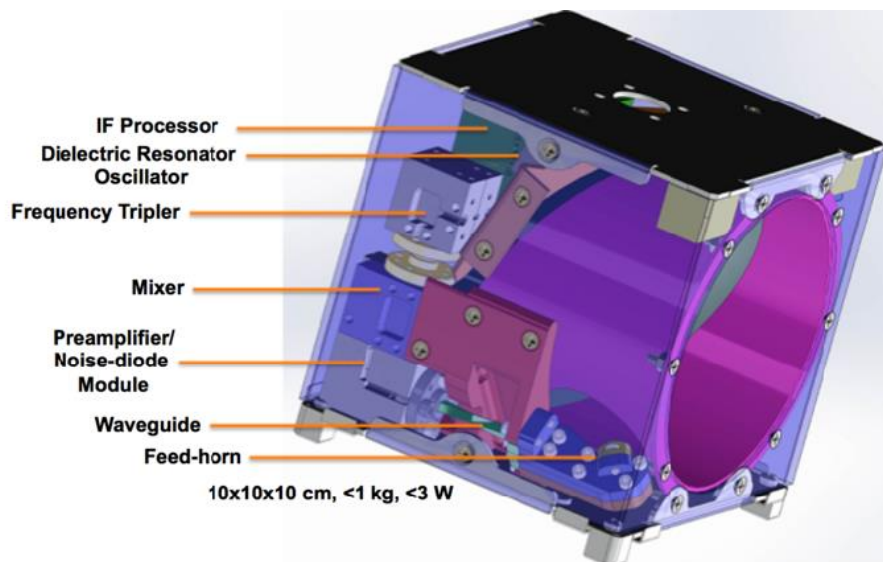
Figure 5: MicroMAS radiometer hardware design (Blackwell, et al., MicroMAS: A First Step Towards a Nanosatellite Constellation for Global Storm Observation, 2013)

1.5.2 Microwave Radiometer Technology Acceleration

The Microwave Radiometer Technology Acceleration (MiRaTA) spacecraft seeks to build off of MicroMAS's design successes and expand the mission set with additional functionality. MiRaTA is a 3U CubeSat funded by the NASA Earth Science Technology Office (ESTO) and is currently being designed and built by engineers and students at the Massachusetts Institute of Technology (MIT), University of Massachusetts Amherst, Space Dynamics Laboratory, The Aerospace Corporation, and MIT Lincoln Laboratory. MiRaTA's mission is to collect microwave radiometer and GPS radio occultation (GPSRO) data from Low Earth Orbit (LEO). This data will be used to measure all-weather temperature and humidity in order to improve weather forecasting on Earth. The GPSRO measurements collected by three-element patch antenna array on the zenith face of the spacecraft will be used to calibrate the measurements from the three-band passive microwave radiometers. If the mission proves successful, MiRaTA will advance the Technology Readiness Level (TRL) from 5 to 7 for both the radiometer and GPSRO payloads (Blackwell, et al., 2014).

The same patch of atmosphere must be measured by both the radiometer and GPSRO units in order to achieve the desired calibration of the radiometer instrument. This is achieved by performing the "pitch up" or "pop a wheelie" maneuver shown in Figure 6. The MiRaTA spacecraft initially conducts a microwave sounding with all three bands of its radiometer instrument, after which it immediately "pitches up" to expose the GPS patch antennas on its formerly zenith face to the same patch of atmosphere which it studied using the radiometer. MiRaTA then collects GPSRO data from any occulting GPS satellites at that time before "pitching down" and resuming local-vertical local-horizontal (LVLH) orbit and returning its GPS antenna array to use in orbit determination and geolocation.
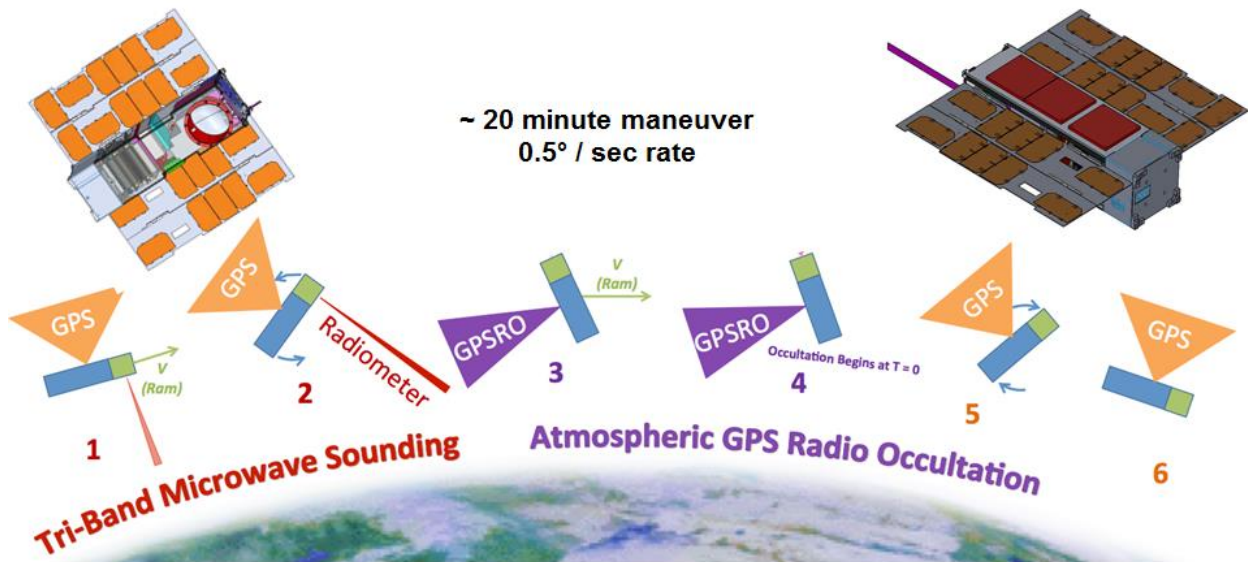
Figure 6: MiRaTA Concept of Operations and Pitch Maneuver (Marlow, et al., 2015)

MiRaTA's overall design consists of a 3-band radiometer combined with a GPS receiver, yielding a larger payload than MicroMAS – just under 2U – with a similar bus. This increase in payload volume required an optimization of the existing bus design on MicroMAS in order to meet the requirements set by the MiRaTA spacecraft. In addition to a decrease in bus volume, MiRaTA requirements also call for a backup radio in addition to a primary radio identical to that used by MicroMAS. The solar panels are in a different configuration, but are from the same vendor – Clyde Space – as those found on MicroMAS, in addition to similar Clyde Space EPS and batteries. The attitude determination and control system is also the same as on MicroMAS, although including a third EHS and programmed to handle a very different set of maneuvers. The zenith face of MiRaTA (when in LVLH) shown in Figure 8 holds the GPS Radio Occultation antenna array and solar cells.
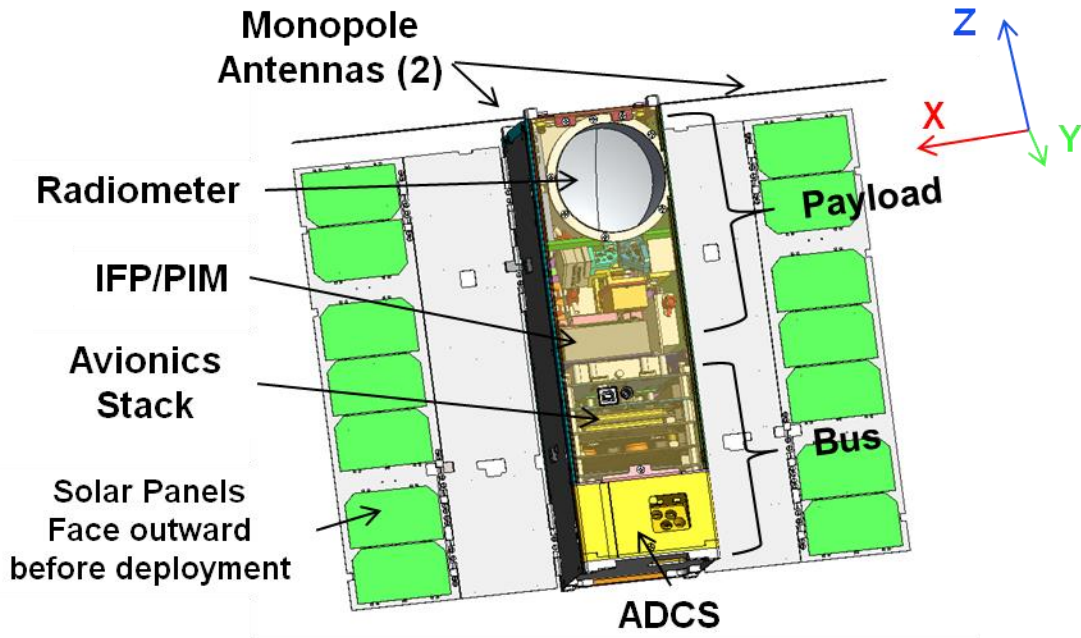
Figure 7: MiRaTA spacecraft design overview, forward face[11]
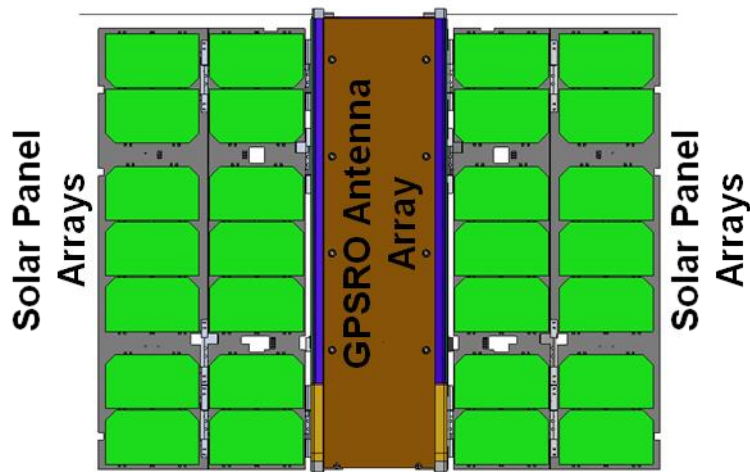
Figure 8: MiRaTA spacecraft design overview, back face[12]

MiRaTA's avionics system, although based on MicroMAS's successful avionics design, required substantial changes in order to meet the requirements set forth for MiRaTA (outlined and discussed in chapter 2.2). Reduced volume, incorporation of a backup radio, and increased memory

---

[11] From MiRaTA Critical Design Review, Lincoln Laboratory, June 3rd, 2015

[12] From MiRaTA Critical Design Review, Lincoln Laboratory, June 3rd, 2015

storage space, among other requirements, drove the design of MiRaTA's avionics system and lead to the design, test, and implementation approach outlined in the rest of this thesis.

1.6 Thesis Roadmap

The remainder of this thesis is to provide the reader with an understanding of CubeSat avionics optimization, using the MiRaTA spacecraft as a case study. In Chapter 2 we will first define "optimization" as it pertains to CubeSat avionics. Once defined, we will further define an approach for applying the principles of optimization to a CubeSat avionics subsystem. Chapter 3 will apply those same optimization principles and analysis techniques to inform changes in the design of the MiRaTA avionics subsystem from its predecessor: MicroMAS. This application will be conducted through critical analysis of the overall avionics stack-up design, circuit board layout, all the way down to individual component selection and integration with the rest of the spacecraft. Next we will apply our optimization approach to a new design: the Micron Motherboard and Radio. Chapter 4 will cover verification of the complete design in acceptance, radiation, structural, and RF testing. Chapter 5 will walk through and critique the results of the tests outlined in Chapter 4. Chapter 6 will discuss conclusions and the future direction of CubeSat avionics optimization.

2 Approach

In this chapter, we will outline our design approach to CubeSat avionics design. We will first define an optimization methodology. Then we will apply that methodology to a predetermined set of requirements in order to then inform both an existing design and future design in the next chapter.

2.1 Optimization

In order to evaluate existing CubeSat avionics designs and inform future designs, a proper understanding of optimization is necessary. There are many ways in which one may approach an optimization problem. Time or processing speed can be a crucial factor in a "shortest path" optimization approach (stochastic complexity). (Rissanen, 1989) Similarly, cost provides a motivation for optimization that results in the smallest possible budget; not just monetarily, but the smallest mass, size, and power budgets as well. When optimizing an avionics design, however, the approach becomes more complicated. While certainly some variables are easily quantifiable (resources, for example), others are not. The combination of these quantitative and qualitative variables forms our metric for optimization: complexity.

2.1.1 Complexity

"Complexity is not easy to define. Worse still, it can mean different things to different people. Even among scientists, there is no unique definition of Complexity." (Neil, 2009) And so we are faced with a challenge: we must attempt to quantify, as best we can, a concept which can neither be properly defined nor, even, properly acknowledged. The result, as we will see, takes a hybrid approach to this problem: quantify what we can, and systematically qualify what we cannot.

2.1.1.1 Effective Complexity

Complexity boils down to information. However, it is not just the *amount* of information which determines complexity, but also the manner in which it is presented. Two cities of similar surface area might have a similar number of roads (amount of information), but their maps may differ in the complexity of their layout (presentation of information). In order to avoid this sort of

confusion, a baseline method of information measurement is proposed: Algorithmic Information Content (AIC).

The Algorithmic Information Content of a system is defined as the fewest possible resources required in order to achieve the requirements of a system S with respect to a universal process U. (Gell-Mann & Lloyd, 1996) The mathematical representation of the AIC is:

$$K_U(S)$$

Returning to the example above, then, each city (system) would require some amount of time (resource) to learn to navigate (process). We would quickly find that the AIC of a city like Washington, DC, with its nice grid network of lettered and numbered roads, would have a lower AIC than that of Boston, MA, with its astonishing variety of one-way streets and six-way intersections. In the case of satellites, the avionics system (system) would require some amount of volume, electric power, processing power, memory, and radiation tolerance (resources) to achieve mission requirements (process).

Information input to determining Algorithmic Information Content comes it two flavors: deterministic and probabilistic. Deterministic information falls under the "information we can more easily quantify" category mentioned in the first paragraph of section 2.1.1. That is, it can be understood as the sum of the independent, identified regularities which comprise a system, effectively measuring the "knowledge" of the system. (Gell-Mann & Lloyd, 1996) Selecting only the deterministic information for use in calculating the Algorithmic Information Content yields the first means of quantifying complexity: the Effective Complexity.

$$\epsilon = K_U(S_D)$$

Where S_D is the set of deterministic components of the system S. The Effective Complexity is what is most commonly referred to in colloquial as well as scientific use of the word "complexity." (Gell-Mann & Lloyd, 1996) The Effective Complexity represents essentially the quantifiable elements of a system's complexity. While the true Algorithmic Information Content of a system is an absolute quantity: the *absolute minimum* resources needed to meet requirements, the Effective Complexity essentially represents a relative Algorithmic Information Content: the *actual* number of resources utilized to meet requirements. This is why both the equation for AIC is used to

measure Effective Complexity, but the Effective Complexity is not necessarily equivalent to the AIC.

2.1.1.2 Entropic Information

But what about the probabilistic or conditional information in a system? What about the elements we cannot easily quantify? These questions are taken into account by the second element in our understanding of complexity: Entropic Information.

Entropic Information is a measure of a system's uncertainty. Taking into account its probabilistic elements, a system's Entropic Information consists of the sum of all resources consumed by "ignorance." The probability of a condition arising ($0 < p_c < 1$) which consumes a conditional quantity of resources R (if condition c occurs, resource sum R_c will be expended) is $p_c R$. Summing all these probabilistic resource consuming events, we find the Entropic Information to be:

$$s = \sum_c p_c R_c$$

This understanding of the Entropic Information as the sum of a system's uncertain elements of complexity serves as a stand-in for a system's qualitative complexities. Although a qualitative phenomenon is certain to have *some* impact, the *degree* to which that qualitative phenomenon impacts a system ultimately depends on probability. Where a deterministic phenomenon has a known, quantifiable impact on resource consumption, probabilistic phenomena by their very nature have a certain but undefined impact on a system's resource consumption.

2.1.1.3 Total Information

Ultimately, any attempt to define a metric for the complexity of a system will become a trade-off between knowledge and ignorance. (Gell-Mann & Lloyd, 1996) Our unit of measurement for knowledge we have chosen to be Effective Complexity. We take all elements of the system which are predictable, measurable, and independent and measure their resource demand to the system in the form of resources. Our unit of measurement for any residual ignorance we have chosen to be Entropic Information. We take all elements of a system which are unpredictable, immeasurable, and conditional and measure their expected resource demand based on a sum of

their probabilities multiplied by the average resource quantity consumed by this group of complexities. The sum of these two values is the Total Information, C

$$C = \epsilon + s = K_U(S_D) + \sum_c p_c R_c$$

From an analytical perspective, it is clear that the closest approximation of complexity depends (at least, as we define it) on a maximization of the Effective Complexity and a minimization of the Entropic Information. In this thesis, we will discuss methods used to gather as much information as possible for use in building "knowledge" in Effective Complexity and leaving as little information as possible to "ignorance" and an Entropic Information approximation. Ultimately, however, as we will see, it is not possible to avoid the qualitative elements that comprise the Entropic Information.

2.1.2 Effective Complexity Applied to Resource-constrained Avionics Design

Maximizing Effective Complexity (as a percentage of Total Complexity) can also reduce risk; the more deterministic a system, the lower the likelihood of failure. For this reason, and in order to better understand complexity in our design, we will seek to conduct as much of our design in the Effective Complexity trade space as possible. We know already our system (S) to be the avionics of a CubeSat (and that system resides within a larger system: the spacecraft). Our process (U) we take to be the mission tasks outlined in the concept of operations. So in order to determine how resources are consumed by performing K_U on S, we need to define our resources.

Table 5: Deterministic Resources in the CubeSat Avionics Trade-Space

Resource	Units	Minimize or Maximize
Mass	g	Minimize
Volume	cm^3	Minimize
Electrical Power	W	Minimize
Processing Power	Hz	Maximize
Cost	$	Maximize
Volatile Memory	kB	Maximize
Non-Volatile Memory	kB	Maximize

Immediately we encounter a problem: not all resources are measured in the same units. We cannot simply declare 1 Watt of power to be interchangeable with 500g of mass. We would not

want to minimize the use of all our resources; some resources are to be maximized, for example, processing power (if that were true, we could launch a brick and call it a day). Our approach to managing this is as follows:

"The scientific notion of Complexity – and hence of a Complex System – has traditionally been conveyed using particular examples of real-world systems which scientists believe to be complex." (Neil, 2009) With this in mind, in order to eliminate the differences in units among our resources, we will normalize resources based on the current state-of-the-art.

For consumed resources (electrical power, mass, volume, cost), we set the minimum COTS consumption to be 1.0. So if a design consumes three quarters the volume of the smallest COTS design on the market, it receives a resource score of 0.75 in volume. For produced resources (processing power, volatile memory, non-volatile memory), we set the maximum COTS production to be 1.0 and invert the factor of our divergence from this maximum. So if a design produces twice as much processing power as the most-powerful COTS design, it receives a resource score of $1 - \frac{1}{2} = 0.5$ (this value is positive and therefore, good). Similarly, if a design consumes four times the volume of the best COTS design, it receives a resource score of $\frac{1}{4} - 1 = -0.75$ (this value is negative and therefore, not good). The result is an optimization algorithm which represents complexity:

$$\epsilon = \sum_n \begin{cases} 1 - \dfrac{R_x}{R_n} \ , & R_x : minimize \\ \dfrac{R_x}{R_n} - 1 \ , & R_x : maximize \end{cases} \tag{1}$$

Where n is the number of resources considered (for this thesis, $n = 5$). R_n is the number of resources consumed by the design measured in the same units as R_x: the number of resources consumed by a representative state-of-the-art system (whether that's a maximum or minimum value). A negative sum indicates that the design is *less optimal* than the standard design to which it is compared. A positive value of ϵ indicates a *more optimal* design, and the degree to which it is more optimal indicated by the size of ϵ. Returning to our previous examples, ϵ would equal 0.5 if processing power were the only resource considered in a design, and ϵ would equal –0.75 if only volatile memory were considered. Taken together, epsilon would equal -0.25, an overall negative

value, indicating a net loss in design optimization. This equation informs optimization by measuring Effective Complexity: the first method of our approach to design.

2.1.3 Entropic Information Applied to Avionics Design

Equation (**1**) takes care of the Effective Complexity. But Entropic Information remains. There are two elements which comprise Entropic Information that, although understood in concrete metrics, remain unquantifiable in the realm of CubeSat avionics design: time and difficulty. Time may be measured in seconds, minutes, or years, but in the context of design it is difficult to capture. It takes time to learn a new programming language, to integrate with the other components of the spacecraft, and to assemble circuit boards at a facility with the resources you lack. An attempt to measure these times could provide insights into the CubeSat design process, but it cannot be applied in a quantitative sense. The "human factor" is too strong. It may take some engineers longer than others to learn a new programming language, different payloads have different interface schemes, and some CubeSat manufacturers have access to better facilities than others. Difficulty, like time, is also unquantifiable. What is difficult for one person may be simple for another. Where the "human factor" is involved, we must, unfortunately, deem those elements Entropic Information.

The impact of the Entropic Information is, we hope, small. If a majority of the complexity of a design is defined by its Effective Complexity, we can pass judgement on the Entropic Information only in the event that we wish to compare two designs (or design decisions) with very similar values of ϵ.

2.2 Requirements

Alongside our optimization equation, we need a set of standards to which we design. That is, we need requirements to answer the question "what is good enough?" while we minimize and maximize our resource consumption and production (respectively).

2.2.1 MiRaTA avionics required functionality

Table 6: MiRaTA Avionics Hardware Requirements

ID	Requirement	Description	Justification	Verification

1	CubeSat Design Specs	The avionics subsystem shall comply with all CalPoly CubeSat and P-POD standards	Must comply with CubeSat requirements	Analysis and Test
2	Watchdog Timer	The Avionics subsystem shall implement a hardware watchdog timer	Prevent mission failure for single fault	Demonstration
3	Powered Temperature	The avionics subsystem shall operate both powered and unpowered within the operational ranges specified by thermal "Component Selection" requirement	Environmental survival	Analysis and Test
4	SWaP	The avionics subsystem shall comply with allocated size, weight and power (SWaP) limits	Mechanical interfaces	Inspection
5	Interface Controls	The avionics subsystem shall provide required electrical power and data connections to onboard electronics, as well as ground station, in accordance with the ICD	Success of scientific payload	Demonstration
6	PIM	The avionics subsystem shall be capable of 2-way communication with the Payload Interface Module (PIM)	Central processing using known system from MicroMAS	Demonstration
7	Buffer	The avionics subsystem shall be capable of buffering received data from peripheral sensors until the communications system can accept it	Avoid dropping packets or data for sake of integrity of scientific mission	Demonstration
8	Time Resolution	The avionics subsystem shall have a timestamp counter resolved to the nearest microsecond and within payload drift requirements	Real time operation	Demonstration
9	Deployables	The avionics system shall be capable of deploying all deployable mechanisms	PPOD requirements mandate deployment after stability in orbit	Demonstration
10	Radiation	The avionics system shall tolerate radiation exposure for the duration of the mission without loss of functionality	Space radiation in Low Earth Orbit (LEO)	Test
11	Backup Radio	The avionics system shall incorporate a backup radio with at least 100 kbps downlink data rate	Redundancy of communication systems	Test

These requirements listed in Table 6 were developed at the beginning of the project, and so reflect intended goals without in-depth knowledge of specific metrics of success. In order to meet the needs of our optimization algorithm, we backed out from these requirements a simplified, quantitative table of values to which we must design.

Requirements 1 and 4 are similar in their relevance to size, weight, and power of the spacecraft. The 3U CubeSat package into which the entire spacecraft must fit limits the overall spacecraft volume to 100mm x 100mm x 300mm. Not all of this, however, may be taken up by the avionics system. If MicroMAS' payload were applied to MiRaTA, it would take up 1U, and a typical COTS attitude control system takes up another 0.5U, so a more realistic limit we may place on ourselves is to fit within the remaining 1U: 100mm x 100mm x 100mm. The weight (more appropriately: mass) requirement for the spacecraft is that it weigh less than 4.3kg in order to comply with the specifications set forth by the most-conservative launch provider.

Power requirements in the sense of SWaP refer to electrical power. For MiRaTA, this value was set at 200mW for avoinics: a flexible maximum based on MicroMAS' avionics power consumption. Transmitting and receiving telemetry and commands from space to Earth, and vice versa, requires higher power outputs and, again inspired by MicroMAS, we set those values at 2W receiving and 10W transmitting.

Requirement 3 and Requirement 10 relate to the space environment. Thermal conditions in Low Earth Orbit (LEO) dictate that all on-board systems not just survive, but *operate* in temperatures from -19ºC to 42ºC. Additionally, the space radiation conditions for MiRaTA's selected orbit expose the avionics system to significant levels of radiation. Assuming 1mm average thickness of aluminum shielding, evenly distributed about the spacecraft (an acceptable assumption), MiRaTA's avionics would be exposed to 9.36krad/yr total ionizing dose (TID). (Aniceto, Lohmeyer, & Cahoy, 2015) This value and others are shown in Table 7.

Table 7: MiRaTA Radiation Analysis (Aniceto, Lohmeyer, & Cahoy, 2015)

Shielding Thickness (mm Al)	Expected Total Dose (rad)		
	Orbit Parameters: 450km by 810km; 97.2 deg.		
	90-DAY Mission	½-YEAR Mission	1-YEAR Mission
0.10	6.47E+04	1.31E+05	2.63E+05
0.50	6.80E+03	1.38E+04	2.76E+04
1.00	2.31E+03	4.68E+03	9.36E+03
1.50	1.29E+03	2.61E+03	5.22E+03
2.00	8.24E+02	1.67E+03	3.34E+03

Requirement 5 (Interface Controls), not easily quantified on its own, instead is quantified by two sub-requirements that facilitate the interface controls requirement: First, the avionics system must possess sufficient volatile memory to simultaneously manage all the peripheral systems it controls and with which it interfaces. This value, based on MicroMAS' similar code structure, we take to be a minimum of 50 kB. Second, the avionics system must have sufficient processing power. Based on software and sampling demands of the sensors necessary on MiRaTA's mission, that minimum processing power is 4 million instructions per second (MIPS). Requirement 8 also is quantified by the same measure.

Requirement 7 leads us to a design with sufficient non-volatile memory as to allow for science data to be kept on-board the spacecraft prior to downlink with a ground station, as well as for commands sent up to the spacecraft to be buffered before execution. From simulations of our intended orbit (450 km by 810 km; 97.2º inclination), we find that just under 1 GB of data is collected over the course of the orbit. The worst-case downlink scenario has MiRaTA dumping that data to a ground station every other orbit, giving us a minimum non-volatile memory of 2 GB (memory required to store uplinked command data is orders of magnitude smaller than downlinked science data).

These simplified minimum and maximum metrics derived from our requirements are shown in Table 8. Requirements 2, 6, and 9 are simple "yes" or "no" checks, ensuring that the avionics system has certain capabilities that are not themselves further quantifiable, and so do not qualify for additional simplified requirements.

2.2.2 Additional hardware requirements for optimization

Two important requirements to consider when optimizing our avionics design which were not included in the official design requirements relate to cost and time. While total program cost for MiRaTA exceeds $3M, this number includes labor costs which leave only a fraction of total cost for avionics hardware. Due to the shared nature of cost (one system's sensor may fall under another system's jurisdiction), backing out a total cost limit for the avionics system alone is very difficult. Our best estimate at a maximum cost we choose to be $30,000, including batteries and the electronic power system which are typically categorized in the power system. Time, similarly, is quantifiable, but carries with it some key qualifications. From "kickoff" until final delivery of the MiRaTA spacecraft is 19 months. How that time is used, however, is up to the team, whose members are often split between multiple projects. Therefore, we tentatively list 19 months as the total time budget allotted to the program.

We have not yet considered mass among our requirements. While mass was not explicitly allocated to our subsystem, we must stay below the total space vehicle mass limits of 4.4 kg. The avionics system mass goal is to stay below 500 g. Mass was left out of any optimization calculations for its reduced importance in already low-mass avionics components and was determined to have a minimal effect as long as common-sense approaches were practiced.

Table 8: Simplified requirement metrics for MiRaTA avionics hardware

Requirement	Limit	Bound
Electrical Power	1000 mW operational	Maximum
Processing Power	4 MIPS	Minimum
Volume	100 mm x 100 mm x 100 mm	Maximum
Non-Volatile Memory	250 MB storage, 256 kB program	Minimum
Volatile Memory	50 kB	Minimum
Cost	$30,000	Maximum
Time	19 months	Maximum
Radiation Tolerance	9.36 krad TID	Minimum

This simplified table of requirements, coupled with our optimization Equation (**1**), give us a coherent approach with which we might assess existing design and inform future design.

2.3 Optimization Equation

And so we are left with the following disparate pieces of information which must be brought together in a final optimization equation:

1. A measure of complexity (Equation (**1**))
2. A standard for resource consumption/production (R_x)
3. Bounds upon those measures ($Min. or Max$).

Our standard for resource consumption depends on the system being evaluated. As we will discuss in Chapter 3, there are at least two ways to define "state-of-the-art" in selecting values for R_x. Similarly for the selection of maximum or minimum bounds on our resources, values will depend on the mission at hand. For example, a 1U CubeSat will have different volume constraints than a 6U CubeSat.

We will also simplify our equation somewhat for application in this work by selecting only 5 of the 8 resources listed in Table 8: Electrical Power, Processing Power, Volume, Non-Volatile Memory, and Volatile Memory. We have chosen to exclude Cost, Time, and Radiation Tolerance due to the difficulty in comparing Cost and Time between missions (discussed in 2.2.2) and the lack of documentation of COTS components' radiation tolerance in TID. (Kingsbury, et al., 2013) These three requirements will be, therefore, considered solely for their bounding value (minimum or maximum) and will not be a part of the summation in Equation (**1**). The number of resources selected will also set the maximum bound of optimization coefficient.

As we follow this approach, we will also keep in mind the inevitable presence of Entropic Information and will consider it in the context of the qualitative features pertaining to design such as difficulty of assembly.

3 Design Analysis

This chapter will focus on the resource constraints outlined in Chapter 2 with regard to two projects: MicroMAS and MiRaTA. MicroMAS's avionics hardware will be only briefly touched upon as a starting point for MiRaTA's design. MicroMAS's avionics hardware will be used as our standard "state-of-the-art" example for R_x values in calculating the complexity of MiRaTA's avionics design. When analyzing MiRaTA's avionics hardware, we will go into more detail about each component in its design. We will then walk through each of the simplified requirements listed in Table 8 and discuss the design decisions affecting each.

3.1 MicroMAS Design Analysis

The first of two ways we will apply our design optimization analysis is through comparing two designs from similar 3U CubeSat missions. We first walk through MicroMAS' overall avionics design and quantify a set of standard R_x values for Electric Power, Processing Power, Volatile Memory, Non-Volatile Memory, and Volume which we can use later in Chapter 4 in evaluating MiRaTA's avionics design.

3.1.1 MicroMAS Design Overview

The avionics design for MicroMAS sits at the center of the spacecraft bus, shown in Figure 9. Following a stack design described in section 1.4.5 with a PC 104 header bus, the MicroMAS avionics consists of six independent circuit boards: a custom Attitude Determination and Controls System interface board, a custom carrier board for the spacecraft's single COTS radio, a battery board with lithium ion batteries manufactured by Clyde Space Inc, a complementary Electrical Power System board also manufactured by Clyde Space Inc, a COTS motherboard manufactured by Pumpkin Inc, and finally a custom top interface board for interfacing with the payload and housing the motor controller assembly.

MicroMAS's avionics design includes many of the benefits of a COTS-custom hybrid system. Using a Pumpkin Motherboard and ClydeSpace EPS and batteries – challenging designs with no room for error – were key decisions which enabled the design of MicroMAS's avionics to be largely completed by graduate students with some mentorship from professional engineers. The

47

decision to use a COTS radio was necessitated by the needs of the mission: the data rate requirements levied on MicroMAS's radio were not within the scope of a university-level project at the time to make a custom radio. The design of three custom boards, however, enabled MicroMAS to support design features it would have otherwise lacked, such as resistance temperature detectors, an inertial measurement unit, coarse sun sensors, thermal knife drivers, and the motor controller vital to mission success. Where MicroMAS suffered, however, was in its use of volume. Large gaps between circuit boards and bulky COTS components like the magnetometer contributed to the over 1U of space consumed by the avionics stack alone. Additionally, unused functionality on the Pumpkin Motherboard contributed to wasted power and volume, even if it saved on cost and development time. (Blackwell, et al., Nanosatellites for earth environmental monitoring: the MicroMAS project, 2012)

After just nine days on orbit, MicroMAS fell silent and no further communications were received from the spacecraft. This setback, in addition to the desire to further optimize MicroMAS' avionics design, contributed greatly to the design of MicroMAS' successor: MiRaTA. Additionally, MicroMAS-2, another improved design based on MicroMAS, is also being assembled.
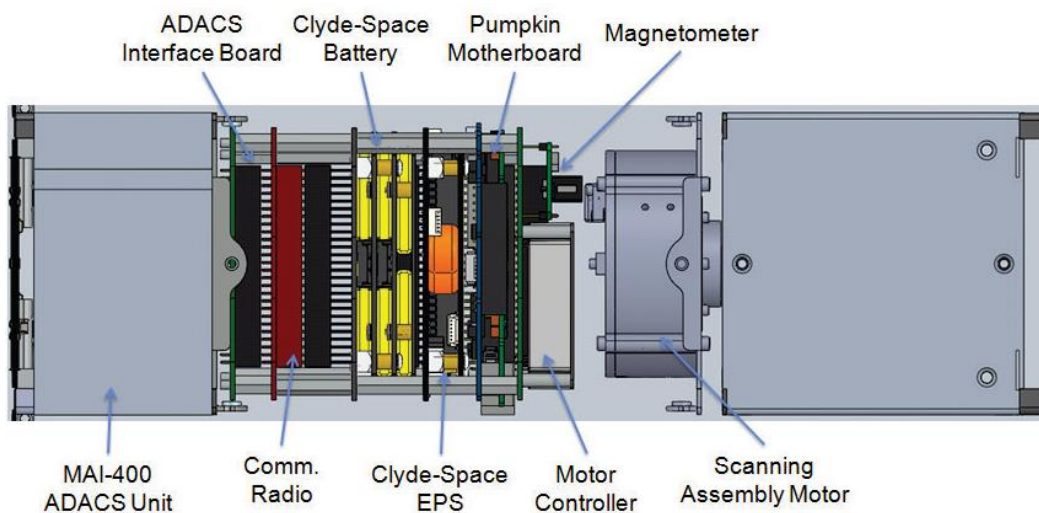
Figure 9: MicroMAS spacecraft bus (Blackwell, et al., Nanosatellites for earth environmental monitoring: the MicroMAS project, 2012)

3.1.2 MicroMAS Design Optimization Analysis

3.1.2.1 Electrical Power

MicroMAS' chosen motherboard, the Pumpkin Motheboard + Pluggable Processor Module, consumes 130 mW of power in operating mode. The combined total of the other three interface boards comes out to 682 mW, which house more power-hungry components like a motor controller and inertial measurement unit. This total – 812 mW – does not include additional peripheral components under the jurisdiction of other systems such as the primary communications radio and the attitude determination and control unit, as well as one-time use systems like the thermal knife drivers.

3.1.2.2 Processing Power

MicroMAS' central processing unit was a PIC24FJ256GB210 microcontroller capable of 16 MIPS – over an order of magnitude higher than the 1.2 MIPS needed by the final MicroMAS flight software. The PIC was physically situated on a pluggable processor module (PPM) plugged (as the name implies) into the top of the Pumpkin Motherboard. This feature enables switching of PPMs for different models, allowing various Pumpkin customers to select from a number of available microprocessors to suit the needs of their mission. The fact that this microprocessor was over-powered meant that no change was required for MiRaTA. However, the additional volume consumed by the PPM was something which was ultimately reduced in MiRaTA's design.

3.1.2.3 Volume

Overall, MicroMAS' avionics design consumes over one third the volume of the spacecraft. The total height of the avionics stack is 130 mm and with boards just under 100mm $\times$ 100mm (a small gap is left around the boards for routing cables), the total volume comes out to 1300 cm^3. A quick inspection of the avoinics stack shows that the spacing between boards leaves gaps. This inefficient use of volume, due primarily to inefficient board layouts and header mating depth requirements, was remedied on MiRaTA.

3.1.2.4 Non-Volatile Memory

MicroMAS' non-volatile memory was contained entirely within a removable SD card on the Pumpkin Motherboard. This allowed for selection of an SD card up to 2 GB in size. An additional 256 kB of memory is available on the PIC microcontroller for program read-only memory (ROM).

3.1.2.5 Volatile Memory

Volatile memory was also contained within the PIC: 98,304 Bytes. Of this volatile memory, less than half was ultimately used even in the most computationally-intensive maneuvers, meaning MiRaTA's design, with a very similar software structure, did not need to increase this value.

3.1.2.6 Radiation Tolerance

Radiation tests conducted by Kingsbury, et al. only validated electrical components (its temperature compensating crystal oscillator, PIC24 microcontroller, serial/differential line transceiver, and SD card) to 8 krad. Because the next-highest radiation dosage tested was 24 krad, and due to the failure of SD cards at 8 krad, we cannot specify a more precise radiation tolerance level than 8 krad TID for MicroMAS avionics components. (2013)

3.1.2.7 Cost

MicroMAS was funded internally by MIT Lincoln Laboratory. In addition to their sponsorship of MIT capstone classes and student research, other MIT resources such as undergraduate research projects and fellowships, as well as faculty time, also contributed to the project. This change of hands makes the total cost of the project from conception to launch very difficult to nail down, but came out to about $2 million.

3.1.2.8 Time

As discussed in 3.1.2.7, the evolution of the MicroMAS project as it developed resulted in a development time that was longer than MiRaTAs and did not have typical need dates and milestones until a launch slot was procured. Design work in MIT classes started in 2010-2011, and delivery to the launch services provider was in March 2014. This number, like cost, is not an

accurate depiction of the project if it were completed by a typical professional engineering organization and comes out to 46 months.

3.1.2.9 Summary

The resource analysis of MicroMAS' avionics design is summarized in Table 9.

Table 9: MicroMAS Design Evaluation for Standardization of Resources

Resource	Value	Bound
Electrical Power	812 mW	Maximum
Processing Power	8 MHz, 16 MIPS	Minimum
Volume	1300 cm^3	Maximum
Non-Volatile Memory	2 GB storage, 256 kB program	Minimum
Volatile Memory	98.304 kB	Minimum
Time	46 months	Maximum
Radiation Tolerance	8krad TID	Minimum

3.2 Application of the Optimization Approach to MiRaTA

We describe the avionics design for MiRaTA in the context of optimization outlined in Chapter 2. MiRaTA's avionics system sought to build upon the successes of MicroMAS and take it a step further. We will analyze the MiRaTA's avionics hardware design as both a whole system and as a family of sub-components.

3.2.1 MiRaTA Design Overview

MiRaTA's avionics design began as an attempt to improve upon the MicroMAS design, maintaining design and component selections wherever possible, in order to achieve maximum efficiency (size, weight, and power reduction) with minimal change. This approach was modified to include an urgent need for redesign to include backup communications capability after MicroMAS' mission was cut short by a communications failure. The need for the redesign and additional capability lead to the decision to attempt a custom-designed motherboard and radio, making optimization an even more crucial element of the already resource-constrained design.

MiRaTA's avionics stack consists of five separate printed circuit boards stacked and connected together on a shared PC 104 electrical bus. This bus allows all five boards to share

power and data lines amongst each other, as well as to pass data lines from below to above (relative to the stack in Figure 10), and vice versa, without the need for additional cables.
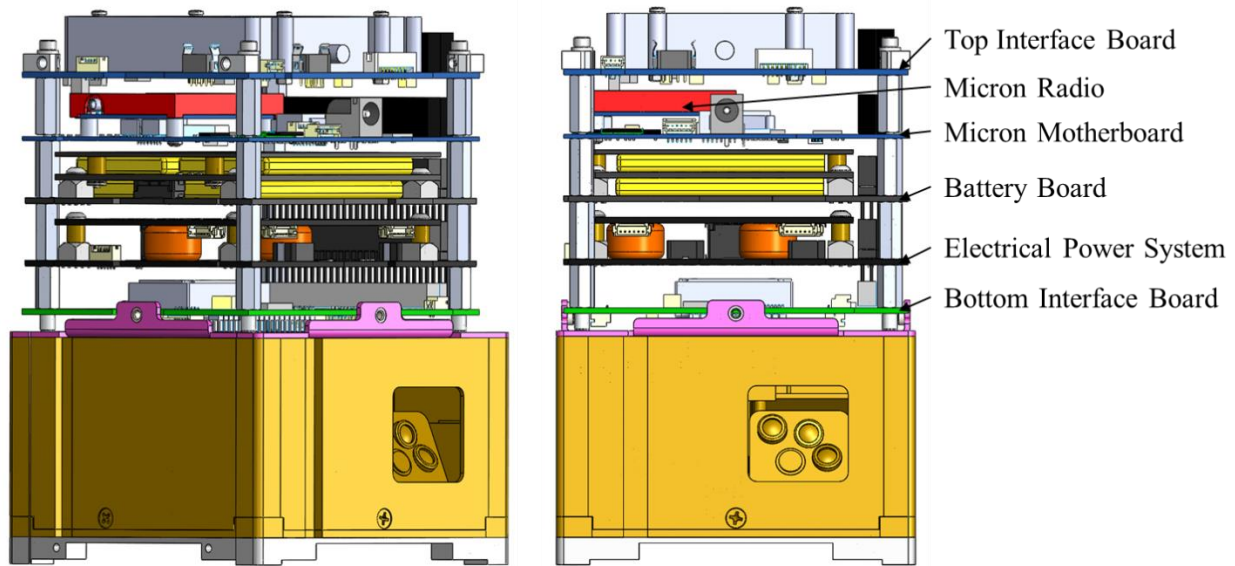
Figure 10: MiRaTA Avionics Stack

3.2.1.1 Electrical Power System

In the middle of the stack are three commercial off-the-shelf circuit boards: the EPS, Battery Board, and Motherboard. The EPS and Batteries were manufactured by Clyde Space, Inc. as standard components nearly identical to those flown on MicroMAS. The tradeoffs between COTS and custom outlined in 1.4.6 ultimately led to the conclusion that the COTS power subsystem, to complement the COTS solar panels manufactured by the same company, was the best path forward. Additional details regarding the design of this power system will not be covered in this thesis.

3.2.1.2 Micron Motherboard

Also in the middle of the stack is the avionics motherboard. The original MiRaTA design used a Pumpkin Motherboard: a COTS component. The motherboard houses the central processing unit, volatile memory, non-volatile memory, and an optional radio for the spacecraft. It represents the core of the avionics, as all data for the spacecraft ultimately passes through or is processed by it. The central importance (data handling and radio communications) and resource harboring

(processing power and memory) nature of the motherboard ultimately lead to the decision to diverge from MicroMAS heritage and design a custom motherboard: The Micron Motherboard.

The addition of the Micron Radio, inspired by the Planet Labs Low Speed Transmitter (LST) radio flown on dozens of Planet Labs spacecraft, was designed to mitigate the risk of a primary radio failure like that experienced on MicroMAS. A common name – Micron – is shared by these two elements (shown in
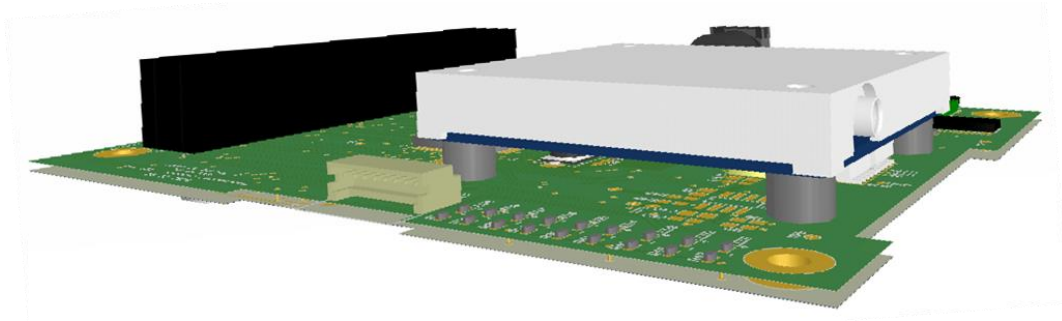
Figure 11) because they are physically paired to one another and were designed to be drop-in replaceable for the Pumpkin Motherboard + Pluggable Processor Module (PPM) + MHX Radio suite, shown in Figure 12, which comes standard with Pumpkin's popular CubeSat Kit.
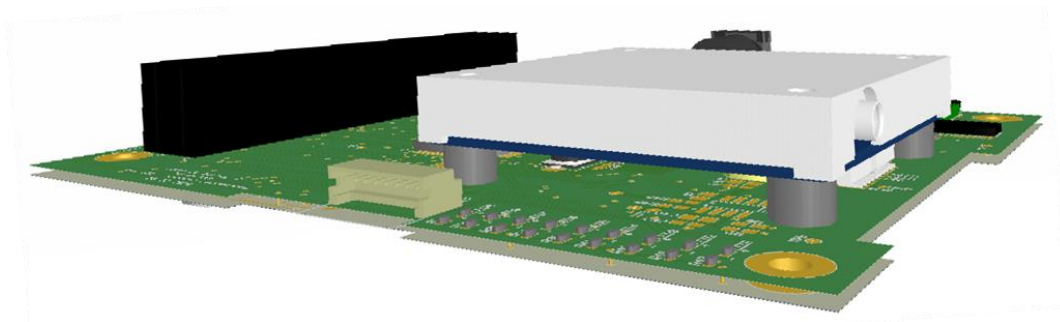
Figure 11: Micron Motherboard + Radio
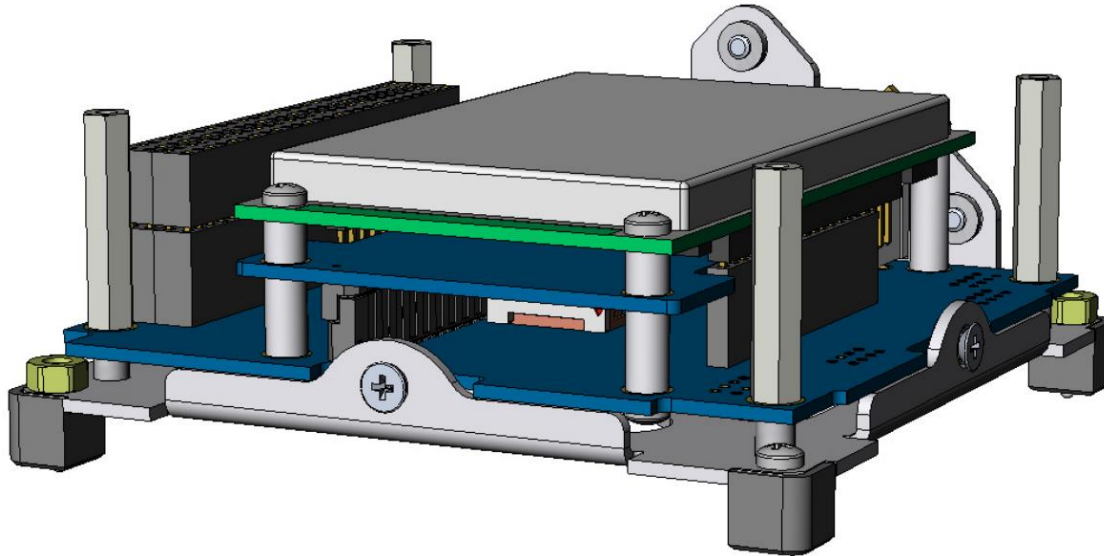
Figure 12: Pumpkin Motherboard + Pluggable Processor Module + MHX Radio[13]

The Micron Motherboard has a 1U CubeSat cross-sectional area with cutouts on each of its four sides to allow for passage of cables and wires perpendicular to it. It is made of 1.6mm thick FR4 Printed Circuit Board (PCB) material. The Micron Motherboard has ESQ series Samtec headers on one of its sides, allowing it to mate with other boards (like MiRaTA's interface boards) using the same PC 104 standard header bus. Four mounting holes, one in each corner, further facilitate stacking of this board with others in the MiRaTA avionics stack. An Omron SS-10GL13 remove-before-flight separation switch – a standard requirement for many spacecraft missions – is also designed into the board with the pin mount penetrating the spacecraft chassis at the same location as the Pumpkin CubeSat Kit.

The central processor on the Micron Motherboard is a PIC24FJ256GB210 microcontroller manufactured by Microchip Inc. This component represents the most sophisticated (in terms of clock speed, memory, and number of I/O pins) version of Microchip's 16-bit, 16 MIPS microcontrollers. Although other microcontrollers were considered with higher values of MIPS than 16, 16 MIPS was considered sufficient for MiRaTA. The PIC is programmed and commanded externally through two separate serial interfaces on the motherboard. Each of these interfaces sits in the same physical location as the USB interface (used only for commanding, not

---

[13] http://www.pumpkininc.com/content/doc/press/Pumpkin_CSDWLU_2008.pdf

reprogramming) on the Pumpkin Motherboard, allowing for it to be not just drop-in replaceable with its COTS contemporary, but an improvement, as it can be programmed in addition to just commanded through those interfaces. The headers for command and programming are Hirose DF13 series headers identical to those used by Clyde Space in numerous CubeSat missions over the past decade.

A JTAG programming interface – also a Hirose DF13 series header – is provided on the Micron Motherboard for debugging. This interface, along with 9 indicator LEDs, allow for improved testing and debugging capabilities over the Pumpkin Motherboard, which currently has no indicator LEDs. 9 low-current (2mA) LEDs were chosen in order to facilitate 8-bit (one byte) coding with one additional bit used as a "heartbeat." While testing on the ground, a 5 V DC power jack provides 5 V directly to the 5 V bus line from which the Micron Motherboard self-regulates its own 3.3 V power plane, independent of the 3.3 V power line throughout the rest of the spacecraft. This isolated 3.3 V plane protects the motherboard from noise or surges on the 3.3 V bus line both during testing and in flight.

In addition to the 256 kB of program memory on the PIC, the Micron Motherboard supports two separate non-volatile memory storage devices. The first of these devices is a Micro SD Card. Where the Pumpkin Motherboard has a full-size SD card slot, the Micron Motherboard, to save on board space, supports only Micro SD cards which, given rapid advances in flash memory technology, store the same amount of data as a full-size SD card. A separate, redundant non-volatile memory storage system comes in the form of four N25Q512A13GF840E NOR flash memory chips, each supporting up to 512 Mbits of data. These chips were wired as a SPI slave network in order to save on I/O pins, using only four total (transmit, receive, slave select, and clock). Having two independent non-volatile memory systems both adds to the total non-volatile memory available, as well as providing a redundant memory source in the event of a failure in one or the other.

Figure 13: Micron Motherboard Component Breakout (credit James M Byrne)

3.2.1.3 Micron Radio

The Micron Radio was designed to operate as a backup radio to transmit at 401 MHz and receive at 450 MHz. High data-rate was, therefore, less important than reliability, which often stems from simplicity. Low power was expected as well (relative to the primary radio), as Radio Frequency (RF) power relates directly with electrical power. While some CubeSat projects turn to the Microhard MHX radio made available through Pumpkin Inc to fit with its Pumpkin Motherboard and PPM, we were looking for something smaller, with greater range, and with lower power. Fortunately, Planet Labs, a private company which launches CubeSats for Earth observation in LEO, had a pre-existing design for a low-speed transmitter (LST) that fit our communications requirements easily. It then became a matter of altering the design of the Planet Labs LST to suit our needs.

The Micron Radio is a 40 mm x 41 mm PCB made of identical FR4 material to the rest of the custom avionics circuit boards. Around its perimeter is a 2 mm width exposed copper pad with grounding vias placed every 2.54 mm, providing a well-grounded footprint for grounding an RF shield surrounding the top of the radio. A conductive gasket is used to conductively and securely

mate the aluminum shield to the ground plane of the radio. All components are placed on the top of the radio, except the Samtec CLM series header connecting it to the Micron Motherboard, in order to utilize the internal ground plane of the radio as the final face of the RF shield.

The Micron Radio's "brain" is a Texas Instruments CC1110 System-on-a-Chip, which provides the processing power of a microcontroller while simultaneously generating an RF signal similar to a stand-alone CC1101 chip. This component, designed for use in consumer electronics from garage openers to amateur radios, is incredibly simple and straightforward to program and operate, making it an ideal platform for a reliable, backup radio. The CC1110 uses an external FOX24 temperature-compensating crystal oscillator to maintain accurate timing in the thermal environment of space.

The transmit signal travels from the CC1110 to an RF1602 broadband SPDT switch which selects either transmit or receive, not both, making the Micron Radio a half-duplex radio. Once past the RF1602 a transmit signal travels to an RF6504 Front-End-Module with a built-in power amplifier to boost the signal strength as well as a built-in low-pass filter to remove any high-frequency noise. The signal then travels through a simple high-pass filter (series capacitor) to remove any remaining low-frequency noise, effectively creating a band-pass filter, and on to a surface mount MMCX plug. An MMCX plug was chosen as the monopole antenna interface for its small size.

The receive signal travels back from the same monopole antenna through the MMCX plug, back through the same high-pass filter, and into the Front-End-Module which, in receive mode (the RF6504 also has an internal Single-Pole Double-Throw (SPDT) switch), simply routes the signal through itself. A received signal next travels through an RLM-23-1WL+ Broadband Limiter which removes any noise that may have leaked onto the receive line from the transmit line. Additionally, this limiter protects the Micron Radio from the more-powerful transmit signal of the primary radio, enabling the Micron Radio to remain powered on at the same time as the primary radio without being damaged. From the limiter, the receive signal next travels through a MAX2640 Low Noise Amplifier (LNA) which amplifies the strength of the signal by 15 dB. The receive signal next travels through the RF1602 broadband SPDT switch before returning to the CC1110 System-on-a-Chip for processing.
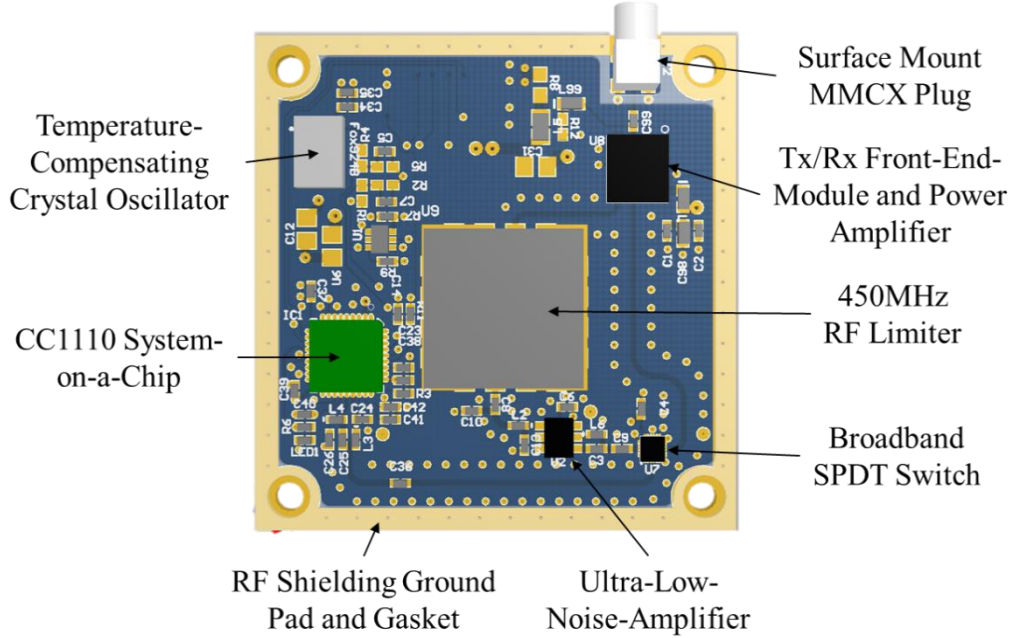
Figure 14: Micron Radio Component Breakout (Credit James M Byrne)

The transmit line of the Micron Radio must have a width chosen to account for the PCB stack-up properties like dielectric, copper weight, and distance between boards, which vary between board manufacturers, and maintain a 50 Ω impedance at 401 MHz – our chosen transmit frequency. The width of a microstrip on the top layer is calculated using the equation **(2)** (Ardizzoni, 2005):

$$Z_o = \frac{87}{\sqrt{\epsilon_r + 1.41}} \ln\left(\frac{5.98H}{(0.8W + T)}\right) \qquad \textbf{(2)}$$

Where Z_o is the impedance of the trace (50 Ω), H is the distance between the trace and the ground plane below it, T is the thickness of the trace, and W is the width of the trace. ϵ_r is the relative permittivity of the dielectric, which can also be chosen if specifically requested to the manufacturer of the PCB. The receive line of the Micron Radio must also be 50 Ω and so its trace width was chosen to match its 450 MHz receive frequency. However, at Ultra High Frequency (UHF) levels, one will notice that impedance is not frequency-dependent. Designs in the GHz range require greater fidelity in their impedance calculations, but for the purposes of the Micron Radio and its chosen frequencies, equation **(2)** was sufficient.

In an effort to reduce noise, digital components (CC1110, oscillator, motherboard interface header) are isolated from RF components (LNA, SPDT switch, Front-End-Module, Limiter, MMCX header) to different areas of the circuit board. No traces associated with digital components travel above or below RF signals, and vice versa. Additionally, the ground plane is split into an RF ground plane and a digital ground plane with a single choke point that prevents signal leakage from one section to the other.

3.2.1.4 Interface Boards

At the top and bottom of the stack are two interface boards, each 4 layers and made of 1.6 mm thick FR4 material. With the attitude control system at the bottom of the spacecraft, the Bottom

Image Removed
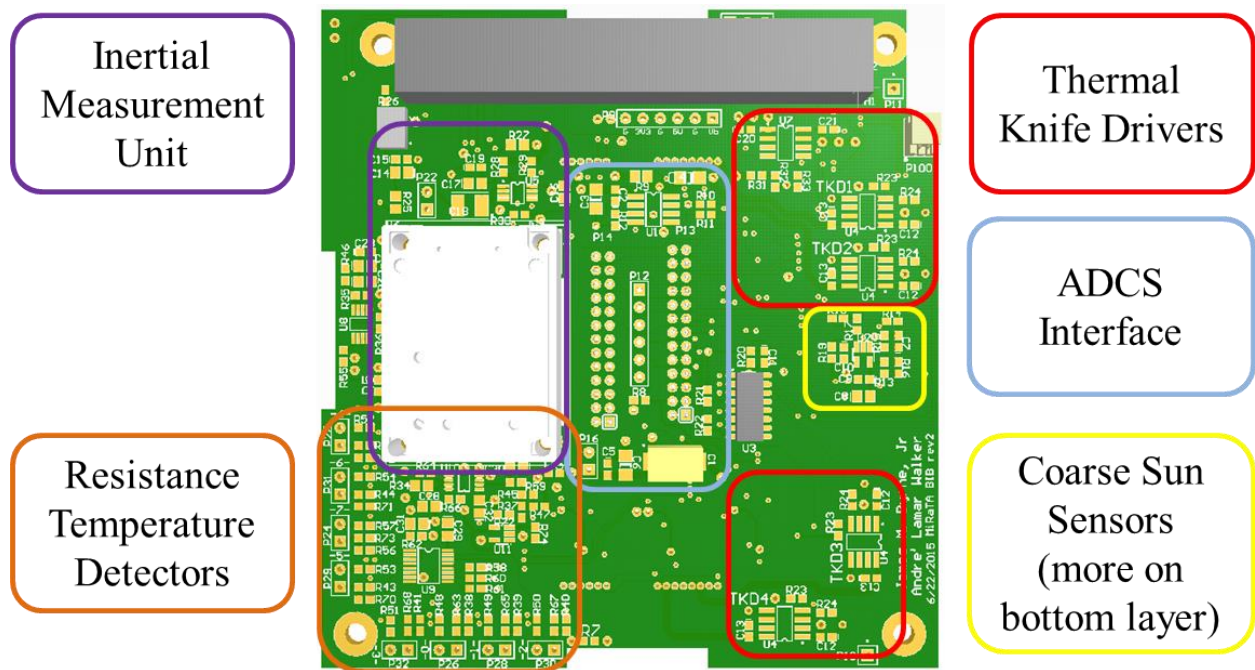
Figure 15: Bottom Interface Board Component Breakout. Sensor circuits are displayed in groups according to color. Barren spaces on the top layer show the location of coarse sun sensor circuitry on the bottom layer. (Credit James M Byrne)

Similarly, the Top Interface Board (TIB) was designed to interface with the Communications and Payload systems. It houses the data circuitry (line transceivers) and power distribution unit for the Radiometer and GPSRO packages, data and power lines for the Earth Horizon Sensor located in the Payload section of the spacecraft, and a redundant set of data and power lines for the backup radio (should it ever need to be placed in the Payload section of the spacecraft as well). The Top Interface Board also serves as the carrier board for the primary spacecraft radio – a function which, in MicroMAS' avionics design, called for a separate PCB. Part of its role as radio carrier board is also thermal dissipation of the primary radio, as it can get up to 50ºC during transmit. To fulfill this role, the TIB has an exposed copper ground pad that the radio connects to via thermally-conductive material. This pad extends to a thermal strap which can then thermally couple the board to the chassis of the spacecraft, creating an even larger heat sink.

Combining the roles of Payload Interface and Communications Interface onto a single board saved considerable volume, detailed later in this thesis. The final circuit on the Top Interface Board was for the magnetometer which, although connected to the ADCS system, needed to be placed far away from the magnets in the reaction wheels in order to avoid interference.

60
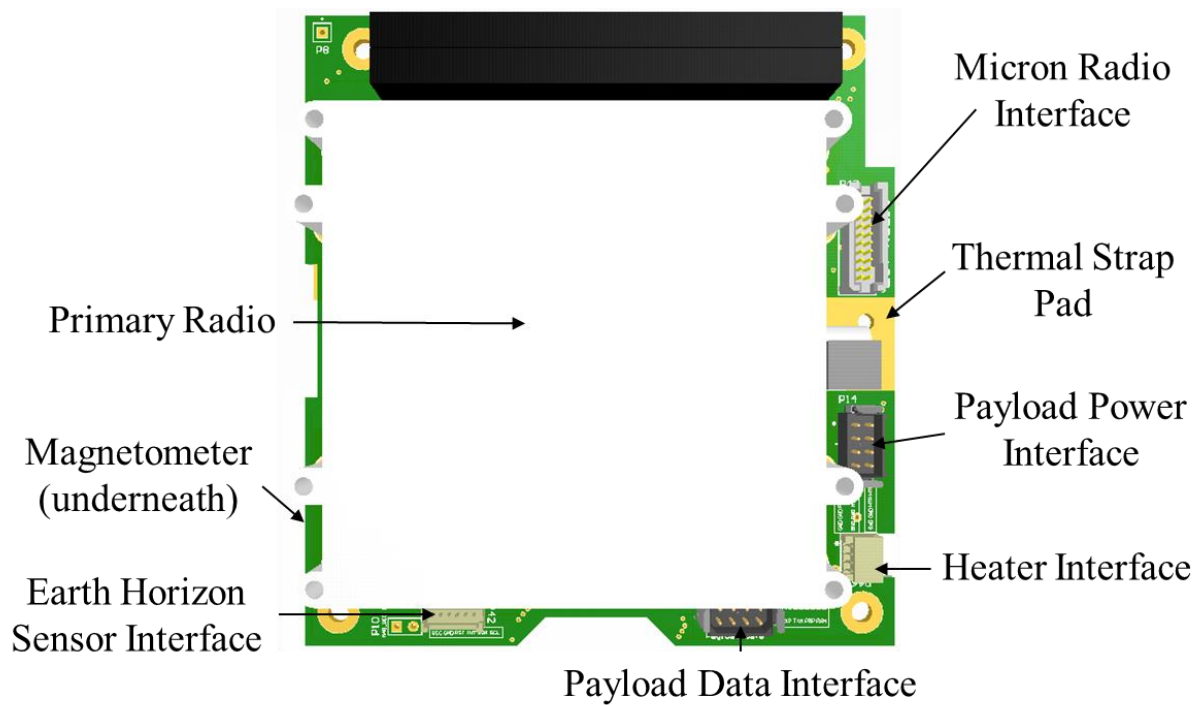
Figure 16: Top Interface Board Component Breakout. Circuits supporting interfaces and magnetometer are on the bottom layer, underneath the board from this perspective. (Credit James M Byrne)

The final avionics stack-up capitalizes on MicroMAS' strengths (processing power, volatile memory, electrical power) and improves upon many of MicroMAS' key weaknesses (volume, non-volatile memory, radiation tolerance). The following section walks through a more detailed analysis at each of these resources and the way MiRaTA's avionics system was designed to optimize their consumption or production.

3.2.2 MiRaTA Design Optimization Analysis

3.2.2.1 Electrical Power

MiRaTA's avionics were designed to consume as little power as possible. Selection of more sophisticated ICs and an intelligent power distribution system contributed greatly to this effort. On the Micron Motherboard, many of the superfluous components found on the Pumpkin Motherboard (such as Universal Serial Bus (USB) interface circuitry) are not found on the Micron Motherboard, saving electrical power. In addition, when operating the interface boards, MiRaTA's avionics system powers on or samples from only one sensor or interface at a time, resulting in power consumed only when necessary, rather than all the time while operating.

A power-conscious design was essential given our chosen orbit and mission requirements. MiRaTA's orbit and high-volume data capture requires additional precautions be taken to ensure the mission remains power-positive. Table 10 shows that, with the addition of a sun-tracking mode, MiRaTA is able to operate power-positive and maintain its "high science operations" profile.

Table 10: MiRaTA Power Consumption – Mode Analysis (Credit Annie Marinan)

Mode	Inhibit	Deploy	Safe	Detumble	Maneuver		Idle	Downlink
Energy Margin	13%	225%	64%	11%	-21%	LVLH	-4%	-18%
						Sun-Track	43%	33%

The decision to implement a sun-tracking mode does not diminish the need for low-power avionics in the bus, as the longer MiRaTA needs to spend recharging, the less time is spent gathering data. For this reason, shared by all systems on the spacecraft, electronics were chosen for their low-power properties and the number of components was minimized where possible.

Power distribution design was also critical to design optimization. The ability to power cycle components and sub-circuits is critical to avoiding standby (also called "vampire") power drain and quiescent current power drain over time. Power switching was designed into the MiRaTA avionics through the use of two different high-side current limit switches: one for high currents (over 250mA) and another for low currents (less than 250mA). These power switches, called Power Distribution Units, perform two other important roles in addition to power switching: fault detection and current limiting. A single PDU (or multiple in series for redundancy) was placed between the main power lines running the length of the avionics stack and the circuit in need of electricity and could be controlled by the main microcontroller on the motherboard.

This power scheme, however, is not without fault. Specifically, the use of a PDU to protect communications hardware holds significant risk. While power cycling, current limiting, local voltage regulation, and fault detection remain essential risk-reduction strategies for the communications subsystem, placing a PDU on the communication system's power line brings with it the question: what should be done when a fault *is* detected and the PDU trips? Without power to the communication system, no command can be sent to reset the PDU and resume operation.

This conclusion is challenged, however, when one considers the use of an automatically resetting PDU or the implementation of a watchdog timer. Many power switches exist on the market which will reset and turn back on after a few hundred milliseconds in order to combat the

risk of a false-alarm trip. We elected to place a resettable PDU on the main power line to the primary and backup radios on MiRaTA.

3.2.2.2 Processing Power

Processing power readily exceeds resource requirements. MicroMAS' required processing power for its bus was only 1.2 MIPS – an order of magnitude lower than the potential of MicroMAS' chosen processor – and MiRaTA's 4 MIPS requirement was still sufficiently below the 16 MIPS that a PIC24F256GB210 can provide, so an improved microcontroller was deemed unnecessary. With a selection of an identical PIC24F256GB210 for the Micron Motherboard, MiRaTA's processing power requirement was expected to be met with no change from MicroMAS.

One may note, however, that processing power being "cheap," so to speak, provides an excellent opportunity to improve our overall optimization score. Why not choose a more powerful microcontroller and exceed requirements by even more? This is where Entropic Information comes in. By using the same microcontroller as was used on MicroMAS, and as is used on numerous other satellite and ground-based microcontroller projects, we were able to eliminate some of the unknown-unknowns in our optimization equation and avoid additional, unforeseen complexities arising from learning a new coding language, starting scripts from scratch instead of using MicroMAS' existing code, and adapting hardware to a new core processor that has no heritage within our Lab. Therefore, the decision was made to keep the PIC24F256GB210 as our bus avionics central processor.

MiRaTA's design to use a simple microcontroller as the central processor for the spacecraft is dependent on a distributed processing system whereby other systems, such as the attitude control, main radio, backup radio, electrical power, and payload system, each had their own microcontroller dedicated solely to the functions of that system. For example, the MAI-400 ADCS system has its own microcontroller driving the reaction wheels and magnetorquers, gathering data from external sensors, and calculating maneuvers, while simultaneously receiving commands and reporting telemetry to the main avionics microcontroller. With every other system on the spacecraft controlled by its own microcontroller, that leaves only higher-level tasking, memory management, and data routing to the motherboard. This scheme enables the use of simpler, less-

expensive, and lower-processing-power microcontrollers in each spacecraft system, including the system at the center of them all: the avionics.

3.2.2.3 Volume

MiRaTA's avionics system made use of a number of strategies to reduce volume significantly from MicroMAS' design. The first of these strategies was the integration of a new PC104 bus header: The BCS-126-L-D-TE. MicroMAS' design used entirely ESQ-39 series headers, identical to those used by CubeSat component manufacturers Clyde Space and Pumpkin (supplies for MicroMAS' EPS, Batteries, and Motherboard, respectively), to form the backbone of its avionics stack. Because ESQ-39 series headers have a specific mating depth illustrated in Figure 17, no standoffs less than 16 mm could be safely used to physically connect the boards. By using a BCS series header on MiRaTA's Bottom Interface Board, we are able to insert the board above it (the EPS – identical to the one used on MicroMAS) an additional 4mm, saving 1.3% of the total volume of the spacecraft, nearly 3% of the total volume of the bus, and 4.5% of the volume of the avionics stack by this simple design decision.
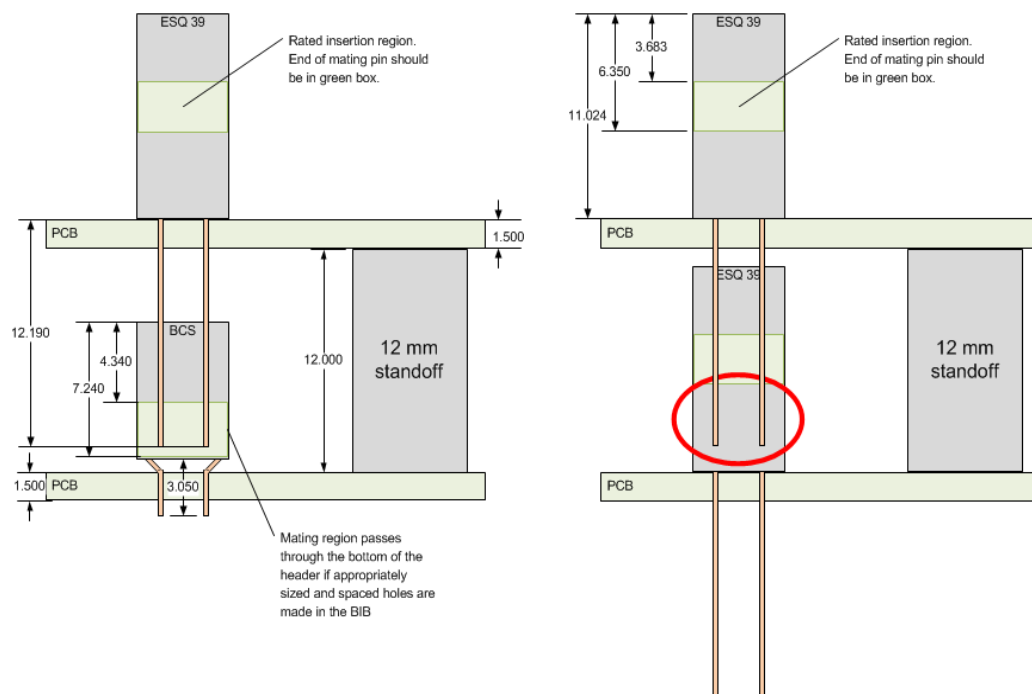
Figure 17: MiRaTA PC 104 Bus Header Mating Diagram. Units are in mm. (Credit James M Byrne)

The total number of boards used in MiRaTA's avionics stack was also reduced. For simplicity, MicroMAS' avionics separated the primary radio on its own carrier board, with simple supporting circuitry. Although this radio took up nearly the entire top layer of the board, the bottom layer was barely utilized. This unused real-estate was used in MiRaTA's avionics stack to house most of the components of the Top Interface Board. This decision to share a single board between TIB components and radio components saved additional space by allowing the radio to move to the top of the stack. Since the radio is 18 mm tall, a standard ESQ header would not mate properly with the board below it if the radio board were internal to the stack without using a bulky extender header that would increase board spacing to 24 mm. Immediately, the decision to move the main radio to the Top Interface Board reduces the overall height of the stack by: 18 mm (extra board thickness + standoff height) + 6 mm (additional space if radio were internal to the stack) = 24 mm.

The remaining components on the MicroMAS TIB that could not fit with the addition of the main radio – the IMU, RTDs, and their supporting circuitry – were relocated to the BIB. In order to accommodate this increase in components, the Bottom Interface Board underwent a complete layout overhaul. The board space was separated into different regions of the board for different sub-schematics. This allowed for efficient routing of traces and less potential for cross-talk among different sensors and systems. However, although additional circuits were added to the BIB, the total number of components slated for inclusion on the BIB only increased from 164 to 207. This was due to design improvements such as the reduction in TKDs and more efficient use of noise-reduction circuitry.

3.2.2.4 Non-Volatile Memory

Non-volatile memory was a key area where improvement could take place between MicroMAS and MiRaTA, as electronic data storage technology has existed for years which far outpaces the storage amount and scheme on MicroMAS. MicroMAS' sole source of non-volatile memory, outside the microcontroller's program memory, was in the form of an SD card which could store up to 256 GB of data. MiRaTA's design, in an effort to conserve volume and real estate on the motherboard, incorporated a Micro SD card with storage capacity up to 200 GB.

MiRaTA's custom motherboard – the Micron Motherboard – was designed to improve upon this MicroMAS's by adding a redundant system of NOR flash memory chips summing to 2.048 Gbits of additional storage. 2.048 Gbits was chosen as additional storage based on the

predicted data collection rate of the science payload. Specifically, each orbit, MiRaTA collects just under 1Gbit of data which it then, if weather and orbital characteristics permit, downlinks and transmits in full to a ground station. Just over 2 Gbits of flash memory was, therefore, sufficient to cover two full orbits in the event that a downlink is missed or incomplete.

Available program memory was unchanged from MicroMAS: 256 kB. At the time of the completion of this thesis, the flight software was not yet complete but expected not to exceed even 75% of the total program memory. MicroMAS, with a very similar software structure to MiRaTA, even sharing many identical drivers, utilized only 52% (180 kB) of available program memory (ROM).

3.2.2.5 Volatile Memory

MicroMAS only ultimately needed 36 kB of Random Access Memory (RAM), and with MiRaTA's similar code structure, even a 100% increase in RAM requirements, while implausible, still falls below the maximum allowed 98.304 kB. RAM was more than sufficient and so was not pursued for improvement. Indeed, the built-in "optimization" option on the software compiler was not used, as it was not necessary to meet requirements and conserved no resources that would assist in optimization.

3.2.2.6 Cost

The total cost of MiRaTA's avionics stack is difficult to nail down. MiRaTA's spacecraft bus hardware cost $276,000. Of that, $30,000 was allocated to avionics hardware. However, even after designs were complete and the bus was built, the shared nature of resources among the spacecraft systems made backing out a cost of a single one extremely difficult. For example, wires and cables that connect the avionics to the payload could be considered to fall under either system's jurisdiction.

3.2.2.7 Time

MiRaTA's design timeline was, even by CubeSat standards, very short. From when funds were first available in April 2014 (program re-start with MIT as lead was in Dec 2013), the MiRaTA team had 20 months to deliver a functional space vehicle. As over half of the engineers working on MiRaTA were also graduate students (and some undergraduates), and the remaining

engineers had additional projects to occupy their time, no one working on MiRaTA could fully dedicate 100% of their time to the effort, which makes 19 months a sufficiently "fuzzy" number to remove time from the calculation of design optimization. Additionally, MicroMAS' situation was even more difficult to quantify, as the project developed over time from an undergraduate design project to a graduate student thesis to a fully-funded program led by Lincoln Laboratory. This evolution supports the decision to remove time from our calculations.

3.2.2.8 Radiation Tolerance

MiRaTA's orbit, while still Low Earth, exposes the spacecraft to a considerable amount of radiation. Table 7 displays the expected total ionizing dose of MiRaTA with a given shielding thickness over a period of time, visualized in Figure 18. We took 1 mm of aluminum shielding over a one year mission as our standard for radiation tolerance of MiRaTA's avionics system, meaning all components would need to operate within characteristic values up to 9.36 krad TID. This radiation exposure is nearly an order of magnitude greater than the original expected orbit (MicroMAS' orbit), which would have exposed a spacecraft with the same 1 mm shielding to 1.86 krad over the same one year period.

Expected Total Dose for Orbit Parameters: 450km by 810km; 97.2 deg
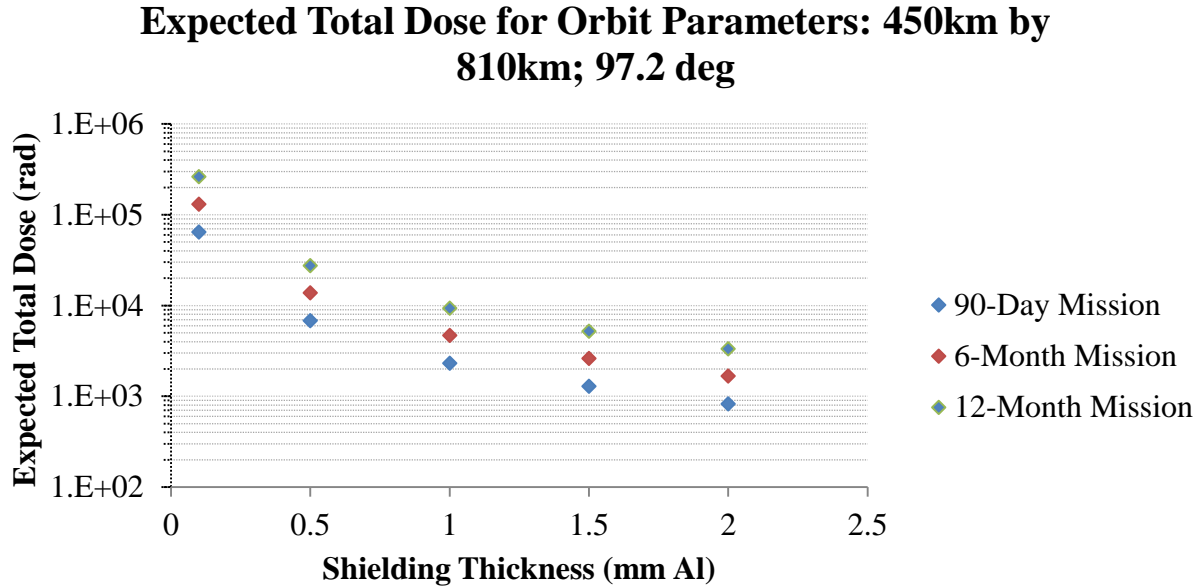
Figure 18: Expected Total Dose of MiRaTA's orbit with varying shielding thicknesses and mission duration times

This significant increase in radiation tolerance required by MiRaTA as compared to MicroMAS inspired three key design decisions. First, MiRaTA's Micro SD cards are industrial grade, meaning they were designed to withstand a greater range of temperature, pressure, and humidity conditions than their standard counterparts on Earth. While industrial-grade and space-grade are different things, industrial-grade Micro SD cards were selected based on an understanding of radiation effects. High-energy electromagnetic waves damage electronics in a similar way that other forces (heating, humidity) do on Earth: they physically alter the molecular structure and chemically alter the molecular properties of the silicon.

The second radiation-inspired design decision was to incorporate a redundant memory storage system in the form of NOR flash chips. The susceptibility of flash memory to radiation is well-documented and known to have caused at least one recent CubeSat mission failure (Springmann, Kempke, Cutler, & Bahcivan, 2012). At the same time, alternative memory storage schemes like Resistive Random Access Memory (RRAM) or Ferro-electric Random Access Memory (FRAM) remain untested or difficult to integrate with the rest of the hardware, respectively. This combination of known susceptibility and lack of viable alternatives led to the decision to incorporate a redundant array of non-volatile NOR flash memory chips in the event that they or the SD card should experience a radiation-induced failure.

The final design decision regarding radiation resistance was the selection of automatically resetting power distribution units on select devices. Although the results of Kingsbury et al. give us confidence in our chosen PDUs, even an unlikely radiation-induced failure was deemed too risky and therefore mitigated by implementing self-resetting PDUs. In the event of a latchup or other failure caused by radiation exposure, the power distribution units supplying electricity to the main or backup communications systems would reset themselves automatically after 182 ms. This design maintains the protective capabilities of the PDUs without risking an accidental power cut due to radiation or other false-positive failure.

4 Design Verification

In Chapter 2 we defined a quantitative methodology for rating the optimization level of an avionics system by comparing its complexity to that of a similar avionics system, as well as an approach for design seeking to minimize specific resources and maximize others. We apply the approach described in Chapter 2 to MiRaTA's design – both overall and component-specific. In this chapter we will determine just how optimized our design is by applying the quantification methodology from chapter 2.

4.1 MiRaTA Verification

The verification process requires first that we characterize our avionics system in terms of the resources it consumes and produces. This characterization is carried out through two test sets: operational testing and environmental testing.

4.1.1 Operational Testing

Operational testing of the MiRaTA avionics system was aimed at characterizing the baseline properties of the avionics system. Operational testing covered expected values of every circuit on the interface boards, as well as recording most of the consumption and production of the resources we have been discussing: electrical power, processing power, volatile memory, non-volatile memory, and volume.

4.1.1.1 Characterization

The first step in operational testing was to characterize individual avionics boards, as well as the stack as a whole. Characterization testing documented the physical and electrical qualities of the avionics system. Boards in the avionics system were first tested individually for baseline SWaP characteristics, and then combined and characterized as a stack.

The first test was the characterization of power planes. A short-circuit test was conducted to ensure the ground plane was not shorted to a power plane. Similarly, each power split-plane's isolation from the others was verified to ensure that, once powered on, each component would receive its expected voltage. Using a power supply, we applied the appropriate voltage(s) to each circuit board and verified that the power split-planes received expected voltages and the ground

plane displayed ~0V. This power plane characterization is the first operational test because it ensures that the greatest risk to circuits during testing – frying components – is mitigated.

The next step in characterization was to apply the appropriate voltages to the power planes on the circuit boards and record their electrical characteristics. Physical characteristics were also recorded in order to verify that volume and mass requirements were met. Table 11 and Table 12 display the results of these physical and electrical characterization tests.

It is important to note that, in order to avoid double-counting the power consumed by the spacecraft and to respect the jurisdictions set between systems, the following components were not considered avionics components in characterizing operating voltage or current values: MAI-400 (ADCS), primary radio (communications), EPS (power), battery board (power), heater (thermal), and earth horizon sensor (ADCS). Although they may be considered under the jurisdiction of other systems, the following components were considered avionics components for the purposes of these tests: Resistance temperature detectors, inertial measurement unit, magnetometer, coarse sun sensor amplifiers, and the backup radio. These components were considered avionics components for their role in gathering telemetry which is processed and packaged directly by the main spacecraft microcontroller. The backup radio is considered avionics for its role as the primary recipient of ground commands for the microcontroller, as compared to the primary radio's role to downlink science data from the payload.

The results of the full avionics stack-up characterization tests are displayed in Table 14.

Table 11: Micron Motherboard and Radio Characteristics

Parameter	Notes	Value	Units
Mass	Motherboard	56	g
	Motherboard + Radio	64	g
Length	Perpendicular to H1 and H2	97	mm
Width	Along length of H1 and H2	91	mm
Height Above Board	Motherboard	11	mm
	Motherboard + Radio	15	mm
Thickness	4 Layer FR4 PCB	1.7	mm
Height Below Board	Tantalum capacitors	3	mm
Remove-Before-Flight Pin Current Limit	Max current applies in normally-closed configuration only	3.5	A
Operating Voltage	Self-regulated 3.3V for Motherboard	5.0, 3.3	V
Maximum Input Voltage	Limited by MAX890 Current Limiter	5.5	V
Voltage Drop from 5 Volt DC input to 5 V Bus Voltage	$I_{IN} = 26mA$	800	μV
Operating Current	5.0V: Motherboard with active PIC	21	mA
	3.3V: Radio (transmit)	136	mA
Reverse Voltage	Through diode in voltage reg. circuit	40	V
Oscillator Frequency	Microcontroller oscillator	8	MHz
	Temperature compensating oscillator	16	MHz

Table 12: Top Interface Board Characteristics

Parameter	Notes	Value	Units
Mass	-	48	g
Length	-	96	mm
Width	-	90	mm
Height Above Board	-	12.5	mm
Thickness	-	1.7	mm
Height Below Board	-	8.0	mm
Operating Voltage	-	3.3, 5.0	V
Operating Current	At 3.3V	1	mA
	At 5.0V	1	mA

Table 13: Bottom Interface Board Characteristics

Parameter	Notes	Value	Units
Mass	-	50	g
Length	-	96	mm
Width	-	90	mm
Height Above Board	-		mm
Thickness	-	1.7	mm
Height Below Board	-	2	mm
Operating Voltage	-	3.3, 5.0	V
Operating Current	At 3.3V	5	mA
	At 5.0V	60	mA

Table 14: Avionics Stack Characteristics

Parameter	Notes	Value	Units
Mass	Includes EPS, Batteries, and standoffs	528	g
Length	Longest component: Motherboard	97	mm
Width	Widest component: Motherboard	91	mm
Height	From top of component below BIB to top of component above TIB	88.5	mm
Operating Voltage		3.3, 5.0	V
Operating Current at 3.3V	When radio is transmitting	150	mA
	When radio is not transmitting	36	mA
Operating Current at 5.0V		82	mA
Operating Power	Max power when radio transmits and all sensors are sampled	Min: 529 Max: 905	mW

4.1.1.2 Functionality

Functionality tests are one complexity level higher than characterization tests. They involve ensuring that data flows properly and command and control from the Motherboard to the Interface Boards, and from the Interface Boards to the rest of the spacecraft, function in accordance with requirements. The result is a series of binary test results: it worked or it didn't. The details of these tests will not be covered in this thesis, as their relevance to optimization rests only in the ability to say "yes, the system works." It is sufficient to state that the avionics system passed all functionality tests.

4.1.2 Environmental Testing

To date, environmental testing of the MiRaTA avionics system took the form of radiation testing.[14] Specifically, based on the radiation environment of MiRaTA's proposed orbit, total ionizing dose radiation tests were conducted in order to validate tolerance to expected values of radiation over a one-year mission. Assuming 1 mm of aluminum shielding on average around the spacecraft, MiRaTA's avionics are expected to experience 9.36 krad of TID. In order to test tolerance at this level and at higher levels (in case of extended mission lifetime and for additional research for future missions), three TID levels were selected for testing: 8 krad, 16 krad, and 24 krad.

4.1.2.1 Test Setup

The test apparatus used for all radiation tests was the Gammacell 220: a cylindrical Cobalt-60 radiation source manufactured by Atomic Energy of Canada Ltd. [1968]

The cylindrical test chamber in the Gammacell 220 supports equal radiation exposure on all sides of the test subject in the chamber, simulating the space radiation environment as accurately as possible. The Cobalt-60 decay releases gamma rays at a predictable, measurable rate, negating the need for an additional dosimeter in the test chamber as well as allowing for direct handling of the tested material immediately after irradiation. (Atomic Energy of Canada Limited, 1968) This is because neutron bombardment results in substantial lingering radioactivity of test subject post-

---

[14] there is future thermal cycling and testing in vacuum planned but those were not in the scope of the current work due to schedule

irradiation and gamma irradiation does not. Test boards were fabricated to support the components tested in a reproducible manner.

Figure 19: Gammacell 220 test chamber (left) and test board (right)

Of note, however, is the lack of energetic particle radiation in this test. The space radiation environment consists of, in addition to gamma radiation, energetic protons, electrons, alpha particles, and other high-mass particles which were not tested or simulated in this experiment due to resource constraints.

4.1.2.2 Component Selection

Components were selected based on two factors: consequences and confidence. That is, if a component failure results in mission failure (high risk profile) and its radiation tolerance is unknown (low confidence), it was tested. Selecting components that qualified under at least one of these criteria avoided a lengthy radiation tolerance test while still mitigating the higher-level risks.

Two smart, low-voltage, P-channel, MOSFET high-side current limit switches were tested: the Maxim MAX892L and the Fairchild FPF2000. These two integrated circuits were chosen in order to better power both low-current devices (MAX892L) and devices demanding higher current levels (FPF2000) while maintaining a low on-resistance. These components have a high consequence of failure, as they serve as PDUs in MiRaTA's avionics design. Some of MiRaTA's payload components require the use of an RS-485 differential-input line transceiver for communication with the bus. A Texas Instruments SN65HVD30DR, which is a 3.3 V full-duplex RS-485 transceiver, was selected to test. This line transceiver was selected for its high consequence of

failure: inability to communicate between the bus and payload, and lack of confidence: it has no documented flight heritage in our expected radiation environment. The last integrated circuit chosen for testing was the ADG452 monolithic, CMOS, single-pole, single-throw (SPST) switch manufactured by Analog Devices. This device was selected for possible use as a low speed 0/3.3 V to ±5 V level shifter – a common circuit in small satellite designs. It met both test criteria. MiRaTA's mission requirements called for a means of storing science data, for hours or even days, prior to downlink. To meet this need, a series of industrial-grade Micro SD cards manufactured by Delkin, San Disk, and Transcend were tested for read and write corruption under the three TID levels. These SD cards not only met test criteria, but they also presented an opportunity to expand the general knowledge of flash memory device tolerance to TID radiation.

4.1.2.3 Component Characterization

In a similar procedure to that outlined by Kingsbury, et al., a number of measurements were used to characterize the components tested before and after irradiation. (2013)

Table 15: Component characterization criteria for TID radiation testing

Component	Characteristic	Abbr.
MAX892L Current Limit Switch & FPF2000 Current Limit Switch	Voltage Limit	V_{LIM}
	Current Limit	I_{LIM}
	ON Switch Voltage	V_{OFF}
	ON Resistance	R_{ON}
SN65HVD30DR RS-485 Line Transceiver	Differential Transmit Voltage	V_{TX+} & V_{TX-}
	Common Mode Voltage	V_{CM+} to V_{CM-}
	Transmit Rise Time	rt_{TX+} & rt_{TX-}
	Transmit Fall Time	ft_{TX+} & ft_{TX-}
	Receive Rise Time	rt_{RX}
	Receive Fall Time	ft_{RX}
ADG452 SPST Switch	Rise Time	rt
	Propagation Rise Time	prt
	Fall Time	ft
Industrial Grade SD Cards: Delkin, San Disk, Transcend	Initialization	Init
	Read Accuracy	Read
	Write Accuracy	Write

4.1.2.4 Experimental Procedure

Prior to radiation testing, all SD cards were tested for initial functionality and read/write capability. This was done using randomly-generated binary files ranging in size from 1 KB to 5

MB for a total of 63.5 MB (the approximate downlink capacity of a single overhead pass for a CubeSat). Accuracy of the read and write on each card was assessed using an MD5 cryptographic hash function checker.

Two of each brand of industrial-grade Micro SD cards were inserted into the test boards, biased to +3.0V. ±5.0V ICs being tested. Separately in the test chamber two additional Micro SD cards from each manufacturer (for a total of six) were placed in an isolated, ESD-proof bag in order to test the cards in an unbiased state.

The MAX892L, FPF2000, SN65HVD30DR, and ADG452 were assembled on the test board, biased to +3.3V, -5.0V, or +5.0V as appropriate and characterized before irradiation. During irradiation, the IC's remained biased. After irradiation, still under bias, the ICs were characterized and compared to their pre-irradiation characteristics.

Using the known decay rate of the Cobalt 60 source and an automatic timer built into the Gammacell 220, three separate test boards with identical components were tested at 8 krad, 16 krad, and 24 krad.

4.1.3 Design Evaluation

The evaluation of the operational and environmental tests are presented in the below subsections, divided into our standard resources outlined first in Chapter 2. After presenting each resource value, we first verify whether it meets our simplified requirements listed in Table 8. Then we calculate an optimization coefficient, ϵ, again using equations from Chapter 2, which will help us quantify the level of our optimization.

4.1.3.1 Electrical Power

From Table 14, we calculate power by multiplying current by voltage for our two voltage levels to yield a total power consumption of 529 mW for MiRaTA's avionics while in operational mode. This total power consumption is significantly lower than the 1000 mW operational power requirement listed in Table 8. Therefore, we can verify, through testing, our electrical power simplified requirement.

Taking MicroMAS' avionics operational power consumption as our standard value (R_x), and noting again that power is a resource intended for minimization, we are able to calculate an optimization score for MiRaTA using equation (**1**)

$$\epsilon_{Electrical\ Power} = 1 - \frac{R_x}{R_n} = 1 - \frac{529\ mW}{812\ mW} = 0.350$$

4.1.3.2 Processing Power

Processing power we know from the specifications of our chosen microcontroller. The PIC24FJ256GB210 operates at a 32 MHz clock rate with 2 cycles per instruction (CPI), yielding 16 MIPS. Immediately we can see that 16 MIPS is four times higher than our requirement of 4 MIPS listed in Table 8.

Once again using MicroMAS' processing power as our standard value for optimization, $R_x = 16\ MIPS$, we note that there was no change in processing power from MicroMAS' avionics design to that of MiRaTA. Therefore, our ϵ value for processing power is:

$$\epsilon_{Processing\ Power} = \frac{R_x}{R_n} - 1 = \frac{16\ MIPS}{16\ MIPS} - 1 = 0$$

4.1.3.3 Volume

The total change in volume between the final MicroMAS avionics stack and the MiRaTA avionics stack is displayed in Figure 20.
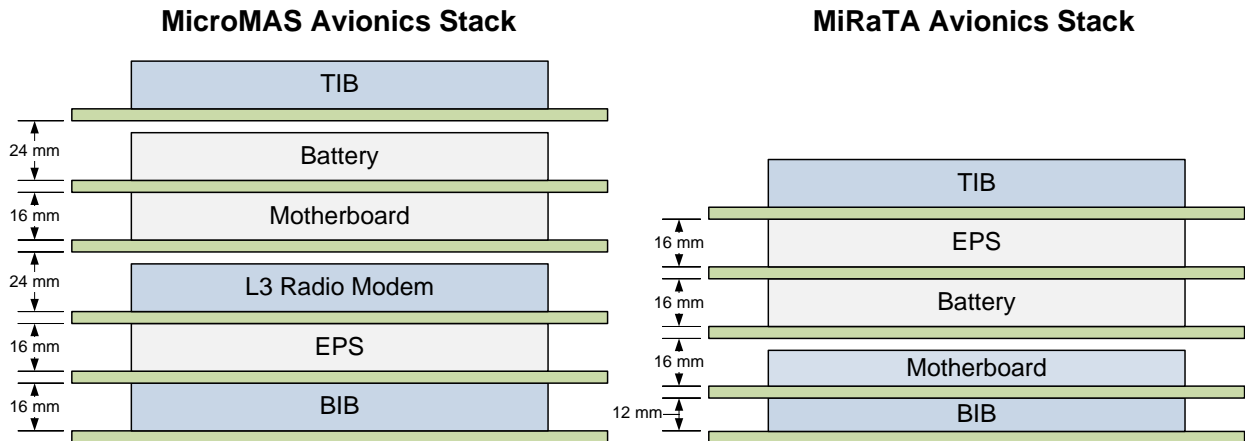
Figure 20: Comparison of MicroMAS and MiRaTA Avionics Stackup Configurations. Custom designed boards are in blue, COTS boards are gray. Each green PCB is 1.6mm thick FR4. (Credit James M Byrne)

The total volume of the MiRaTA avionics stack came out to 100 mm $\times$ 100 mm $\times$ 88.5 mm = 885 cm^3, which is a full 115 cm^3 less than the requirement and 415 cm^3 less than MicroMAS. Calculating an optimization coefficient for volume, we get:

$$\epsilon_{Volume} = 1 - \frac{R_x}{R_n} = 1 - \frac{885 \text{ cm}^3}{1300 \text{ cm}^3} = 0.319$$

4.1.3.4 Non-Volatile Memory

MiRaTA's total non-volatile memory is a sum of two storage capacities: the removable Micro SD card and the permanent NOR flash memory chips. There are four NOR chips with capacity 512 megabits each, summing to 2.048 gigabits, or 256 MB. This value alone is sufficient to meet the 250 MB non-volatile memory storage requirement set in Table 8. However, we have additional, redundant storage capability in the Micro SD card up to 200 GB. (Andrade, Press Releases, 2015) Our total storage, therefore, comes out to 200.256 GB – well above the simplified requirement.

Generating an optimization coefficient from this value requires first calculating MicroMAS' non-volatile memory storage capacity. Because MicroMAS' avionics design incorporated the Pumpkin Motherboard, it had room for a full-size SD card, boosting its non-volatile memory storage to 256 GB: well *above* MiRaTA's non-volatile memory storage capacity. (McCormick, 2014) The result is our first negative optimization coefficient:

$$\epsilon_{Non\,Vol\,Memory} = \frac{R_x}{R_n} - 1 = \frac{200.256 \text{ GB}}{256 \text{ GB}} - 1 = -0.218$$

4.1.3.5 Volatile Memory

Volatile memory for the MiRaTA avionics design, via the Micron Motherboard, was 98.304 kB. This value of volatile memory is nearly double the simplified requirement of 50 kB.

Similar to processing power, and for similar reasons (it was not required by the code), there was no change from MicroMAS to MiRaTA. This yields an optimization coefficient of:

$$\epsilon_{Vol\,Memory} = \frac{R_x}{R_n} - 1 = \frac{98.304 \text{ kB}}{98.304 \text{ kB}} - 1 = 0$$

4.1.3.6 Radiation Tolerance

Tables Table 16–Table 19 below display the results of the TID radiation tests on vulnerable avionics components.

Table 16: MAX892 and FPF2000 Current Limit Switch Radiation Test Results

MAX892	8krad		16krad		24krad	
	Pre	Post	Pre	Post	Pre	Post
V_{LIM} (V)	3.12	3.12	3.086	3.15	2.984	3.166
I_{LIM} (mA)	96	96	94.9	96.9	91.8	97.4
V_{OFF} (V)	0.036	0.036	0.033	0.035	0.035	0.036
R_{ON} (mOhm)	375	375	348	361	381	370
FPF2000	8krad		16krad		24krad	
	Pre	Post	Pre	Post	Pre	Post
V_{LIM} (V)	2.11	2.12	2.23	2.239	2.15	2.144
I_{LIM} (mA)	65	65	68.6	68.9	66	66
V_{OFF} (V)	0.055	0.056	0.056	0.057	0.056	0.057
R_{ON} (mOhm)	846	861	816	827	846	864

Table 17: SN65HVD Line Transceiver Radiation Test Results

SN65HVD	8krad		16krad		24krad	
	Pre	Post	Pre	Post	Pre	Post
V_{TX+} (V)	+2.018	+2.093	+2.060	+2.006	+2.061	+2.056
V_{TX-} (V)	-2.025	-2.112	-2.060	-2.048	-2.066	-2.100
V_{CM+} to V_{CM-} (V)	1.948	1.979	1.969	1.920	1.973	1.947
rt_{TX+} (ns)			6	6.8	6	7
rt_{TX-} (ns)			6	6.4	6	10
ft_{TX+} (ns)			7	6.4	7	10
ft_{TX-} (ns)			7	5.6	7	10
rt_{RX} (ns)			6	7	6	14
ft_{RX} (ns)			6	7.4	6	15

Table 18: ADG452 SPST Switch Radiation Test Results

ADG452		16krad		24krad	
		Pre	Post	Pre	Post
Switch 1	rt (ns)	51	58	50	66
	prt (ns)	150	190	150	388
	ft (µs)	14	13	13	1500
Switch 2	rt (ns)	51	58	50	68
	prt (ns)	150	182	150	296
	ft (µs)	14	13	13	1500
Switch 3	rt (ns)	51	58	51	68
	prt (ns)	150	188	148	280
	ft (µs)	13	13	13	1300
Switch 4	rt (ns)	51	58	56	66
	prt (ns)	150	182	149	290
	ft (µs)	13	13	13	1300

Although the SN65HVD and ADG452 were not tested completely at 8 krad, their tolerance to 16 krad indicates that an 8 krad test was not necessary and so was not conducted.

Table 19: Industrial Grade SD Card Radiation Test Results

ADG452		16krad			24krad		
		Initialize	Read	Write	Initialize	Read	Write
Delkin	Bias	Pass	Pass	Pass	Pass	Pass	Pass
	Bias	Pass	Pass	Pass	Pass	Pass	Pass
	No Bias	Pass	Pass	Pass	Pass	Pass	Pass
	No Bias	Pass	Pass	Pass	Pass	Pass	Pass
San Disk	Bias	Pass	Pass	Pass	Pass	Pass	Pass
	Bias	Pass	Pass	Pass	Pass	Pass	Pass
	No Bias	Pass	Pass	Pass	Pass	Pass	Pass
	No Bias	Pass	Pass	Pass	Pass	Pass	Pass
Transcend	Bias	Pass	Pass	Pass	Pass	Pass	Pass
	Bias	Pass	Pass	Pass	Pass	Pass	Pass
	No Bias	Pass	Pass	Pass	Pass	Pass	Pass
	No Bias	Pass	Pass	Pass	Pass	Pass	Pass

These test results show that all of our components of concern can tolerate up to a maximum of 16 krad TID, verifying our simplified requirement that components withstand a minimum of 9.36 krad TID.

MicroMAS' maximum 8 krad TID tolerance, due to its selection of line transceivers with charge pumps, gives us a positive optimization coefficient:

$$\epsilon_{Radiation} = \frac{R_x}{R_n} - 1 = \frac{16 \text{ krad}}{8 \text{ krad}} - 1 = 1.000$$

4.1.3.7 Optimization Results

Table 20: Results of Optimization Analysis for MiRaTA Avionics Design

Resource	Optimization Coefficient
Electrical Power	0.350
Processing Power	0.000
Volume	0.319
Non-Volatile Memory	-0.218
Volatile Memory	0.000
Radiation Tolerance	1.000
Total	**1.522**

Our final optimization value for the MiRaTA avionics design is a positive value: 1.522. This result, other than its sign (positive means net gain in optimization), means little by itself. Its meaning and utility is discussed in detail in the next chapter.

5 Discussion and Design Critique

5.1 Discussion

5.1.1 Optimization Discussion

The final side-by-side comparison of resource consumption/production of MicroMAS and MiRaTA avionics is shown in Table 21.

Table 21: Resources consumed and produced by MicroMAS and MiRaTA

Resource	MicroMAS	MiRaTA
Electrical Power (mW)	812	529
Processing Power (MIPS)	16	16
Volume (cm^3)	1300	885
Non-Volatile Memory (GB)	256	200.256
Volatile Memory (kB)	98.304	98.304
Radiation Tolerance (krad)	8	16

The design of a custom motherboard for MiRaTA contributed significantly to the resource optimization of MiRaTA's design. Table 22 shows a side-by-side comparison of the custom-designed Micron Motherboard's characteristics and those of the commercial off-the-shelf Pumpkin Motherboard.

A cursory glance at Table 21 and Table 22 provides sufficient support to the conclusion that MiRaTA's avionics design is indeed optimized, in our resource-driven definition of the term, over MicroMAS. However it is our optimization coefficient – 1.522 – which provides us with a *quantifiable* metric for just how far that optimization went.

It is difficult to use the term "optimized" when comparing a sample size n = 2. Optimization implies that one design outpaces *several* others. When comparing only two designs, to say "A is better than B" makes more sense than to say "A is optimized over B." Therefore, what we have achieved in this thesis, because we have only compared two designs, is closer to the former. But we have done more than just that. In order for one to ever say "A is optimized over B," a standard

procedure – a protocol with quantifiable metrics – is needed. That protocol (resource comparison) and that metric (optimization coefficient) we have also established in this thesis.

Table 22: Micron vs Pumpkin Motherboard Comparison

Parameter	Micron	Pumpkin	Notes
Mass (g)	56	88	Significant reduction in structures
Length (mm)	97	96	To match TIB and BIB
Width (mm)	91	90	To match TIB and BIB
Height Above Board	15	12.5	Includes Micron Radio
Thickness	1.7	1.6	
Height Below Board	3	3.5	
RBF Pin Current Limit (A)	3.5	10	Pumpkin value probably inaccurate
Operating Voltage (V)	5	5	
Maximum Input Voltage (V)	5.5	5.5	
Voltage Drop from 5 Volt DC input to 5V0 Bus Voltage (μV)	800	1100	
Operating Current (mA)	18	26	May surge when flash is accessed
Operating Power (mW)	90	130	
Reverse Voltage (V)	40	40	
Oscillator Frequency (MHz)	8	8	

It is outside of the scope of this master's thesis to acquire and analyze detailed records of other similar CubeSats, but we recommend future engagement with teams that have produced similar spacecraft such as the RACE CubeSat (Lim, et al., 2013), PolarCube (Weaver, et al., 2012), and IceCube (Wu, et al., 2015). It's difficult to know if 1.522 is "a lot" or "a little." This draws us to conclude that the value of an optimization coefficient is dependent on the number of designs to which it might compare. Our work in this thesis, therefore, is of value primarily groundwork upon which the MIT Space Systems Lab might continue to develop its CubeSat program, building and improving upon avionics design with each successive spacecraft, seeking to maximize production of some key resources and minimizing consumption of others. With each successive design, an optimization coefficient calculated using the methodology outlined in this thesis can be used to inform engineers about the extent to which a design has been improved (within some error bounds, dictated by the influence of Entropic Information)

5.1.2 MiRaTA Avionics Design Discussion

MiRaTA's avionics design improved upon MicroMAS's avionics in volume, electrical power, and radiation tolerance. These resources were deliberately chosen for improvement based on the constraints set by MiRaTA's mission. The presence of a larger payload section (driven by the addition of a new sensor: a GPS-RO package) decreased the allotted volume to MiRaTA's bus. The pre-set size of the ADCS unit meant, therefore, all new payload volume (relative to MicroMAS) would come from volume previously allocated to the bus avionics. Electrical power is often of concern to spacecraft designers, as the nature of solar power frequently requires periods of eclipse during which the spacecraft is operated solely off of battery power. This ever-present constraint, in addition to MiRaTA's power-hungry payload section (as compared to MicroMAS) drove the design of the bus avionics to lower electrical power consumption. A combination of hardware (efficient components, minimal resistance, etc) and software (power-off to components when not in use) allowed us to decrease power consumption of the avionics by 283 mW on average. An increase in radiation tolerance was also mission-driven. CubeSats are often launched on rockets with additional payload space that would otherwise be filled with ballast or left empty. This decreases the cost of launch and improves launch efficiency, but also limits the possible orbits to those desired by other, often-times more radiation-tolerant satellites with which the CubeSat shares the launch system. This is precisely what happened with MiRaTA. A higher, more elliptical orbit exposes MiRaTA's avionics to greater doses of radiation over the same period of time as MicroMAS, necessitating the testing and selection of more radiation-tolerant components, driving also our total radiation tolerance to 16 krad.

There were two resources which MiRaTA's avionics design left unchanged from MicroMAS: non-volatile memory and processing power. This was due primarily to the desire to maintain the same microcontroller from one project to the next. In doing so, software could remain similar and decreased the amount of new learning and work needed on new code. This decision quantitatively has no effect on our optimization coefficient, but it does has a qualitative impact on the design. By apparently doing nothing (not changing microcontrollers, even for a more powerful one), we effectively save *time*: a key resource we did not model in our quantitative analysis. We relegated time to entropic information status outlined in section 2.1.1.2, meaning its impact on optimization, while not strictly quantifiable, is nonetheless present, and therefore must be

considered. This leads us to list "time" spent on MiRaTA as an improvement upon MicroMAS, although we cannot assign a quantitative value to that improvement.

There was one resource in MiRaTA's avionics design which took on a negative optimization coefficient value (indicating a retrogression): non-volatile memory. This was due to a nuance in our optimization equation: an absence of diminishing returns. MicroMAS used a full-size SD card for memory storage, enabling it to store up to 256 GB of data plus additional storage on the primary radio. MiRaTA, with its Micro SD card paired with four NOR flash memory chips, could store only 200.256 GB. While these numbers do show an advantage in favor of MicroMAS's avionics design, the advantage is incredibly small. Neither MiRaTA nor MicroMAS were intended to store more than 1 GB of data on the spacecraft due to the limited downlink data rate (more data stored on-board would have taken multiple downlinks and several days to fully return to ground). Any storage capability greater than 1 GB, therefore, is of reduced value.[15] This diminishing return was not incorporated into the optimization approach we use in this thesis. Additionally, MiRaTA's redundant memory storage systems – an SD card and an independent flash memory bank – was not considered any more beneficial (optimized) than a single memory storage scheme with storage equal to the combined capacities of the two independent systems. This neglect of risk-reduction through redundancy was a conservative decision, as no quantitative benefit could be attributed to this system, relegating risk-reduction, like time, to the realm of Entropic Information.

5.2 Design Critique

One may presume that mission differences between MicroMAS and MiRaTA dictated differences in components required by the avionics system, but given the similarity of the two missions, any component differences (for example: absence of a motor controller on MiRaTA) were simply the result of superior design (a full-spacecraft "pitch up" maneuver instead of a dual-spinner), rather than the result of good fortune in mission requirements. The MiRaTA avionics

---

[15] SanDisk has increased SD card capacity by 1,000 times in just over a decade, which means that MicroMAS' perceived advantage in non-volatile memory storage is largely negated by advances in flash memory technology. Indeed, in just the two years between MicroMAS and MiRaTA's design completion, SD card capacity doubled from 256 to 512GB. (McCormick, 2014)

stack incorporates a backup radio (the Micron Radio) which, if a commercial equivalent were selected (such as a Microhard Systems Inc. MHX radio), would have surpassed the additional volume needs of MicroMAS' motor controller by 2 mm. We can, therefore, compare MicroMAS to MiRaTA – especially their avionics designs – with confidence.

One valid design critique, however, is the adherence to an "avionics stack." As describe in Chapter 1, an avionics stack is a simple design which uses the concept of a shared header bus carrying shared signals and power lines to and from each circuit board in the avionics system. While this design offers simplicity, structural stability, and compatibility with most commercial off-the-shelf components, it uses considerably more volume than a design which incorporates the avionics into the walls of the spacecraft or distributes boards throughout the satellite wherever and sized however they are needed, instead of adhering to a strict form-factor. With this in mind, however, the amount of volume reduced from MicroMAS to MiRaTA was still significant, even with an avionics stack approach.

Another design decision worth discussing was the use of a daughter board to hold the backup Micron Radio. Figure 21 shows the radio mated to the motherboard. Providing a header and mounting holes on the Motherboard allows for different versions of a radio to be mated with the same standard Motherboard, depending on the needs of the mission. This enables minimal changes, if at all, to the Motherboard in future avionics designs. But it is this very advantage which also brings with it the disadvantage we sought to avoid in the Pumpkin Motherboard: excess volume. The minimal volume design is achieved by incorporating the radio directly into the same 4-layer PCB as the rest of the Motherboard. So we are faced with three possible designs, in order from least to greatest volume: Radio + Motherboard hybrid, Motherboard with Radio daughterboard, and COTS Motherboard with COTS Radio daughterboard. We chose the middle option for MiRaTA because the amount of volume saved was just 4 mm if we had chosen the first, and this minimal change we determined to be worth the added benefit of radio interchangeability.
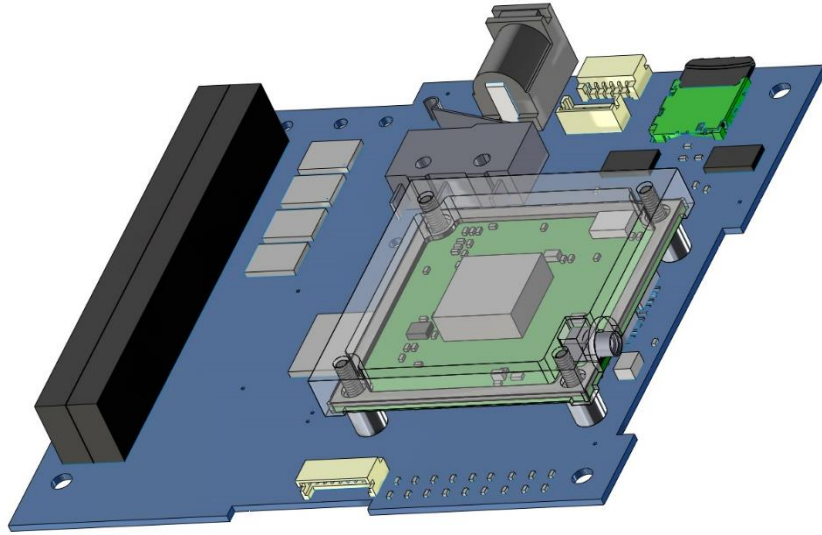
Figure 21: Micron Radio daughter board mated to Micron Motherboard

One final critique for the design is the low data rate (<100 kbps) of the Micron Radio. This data rate may turn out to be too low for science data downlink to ground stations and so the Micron Radio, in its role as a backup radio, falls short of full redundancy with the primary radio. However, in sacrificing data rate, the Micron Radio capitalizes on size (it is, including mating and shield height, approximately 1/3 the volume of the primary radio), power (approximately 1/3 the power of the primary radio), and simplicity (components can be easily swapped out to change operating frequencies). These three benefits, we find, make up for the low data rate of the Micron Radio.

6 Conclusion

6.1 Summary of Results and Findings

The goal of this research was to define an quantitative approach to CubeSat avionics design optimization by maximizing functional resources (processing power, volatile and non-volatile memory, radiation tolerance) and minimizing SWaP resource consumption (such as volume and electric power). The MiRaTA avionics design was used as a case study for our optimization methods and compared to the MicroMAS avionics design to quantify an optimization coefficient which can be used to compare and inform improvements upon future CubeSat avionics designs. The MiRaTA avionics design met all mission requirements and achieved an optimization coefficient value of 1.522. We expect optimization coefficients to range typically from –4 to +4, so this design indicates a modest improvement.

6.2 Application

MiRaTA is only MIT's second CubeSat. It is likely that many more will be designed and launched in the future. The design of these future satellites will likely draw heavily on their predecessors and will therefore share many similarities in their avionics design. As these future satellites are being designed, engineers will likely want to know both how to optimize their avionics, and, once they are complete, just how successful their attempts at optimization were. The result is a system, defined and first applied in this thesis, by which knowledge is quantifiably passed down between iterations and versions of avionics, even in satellites with starkly different mission goals.

It is also this manner of thinking – balancing the conservation of SWaP resources with the availability of functional resources – which we present as an overreaching approach to avionics design. This approach, however, is not limited only to avionics and may be modified to suit additional subsystem design decisions such as communications and ADCS.

6.3 Future Work

There were a number of items which time and resources prevented us from achieving but which remain nonetheless viable pursuits of future work.

6.3.1 Updates to hardware

Over time, functional resources produced by various avionics components come at lower and lower cost in SWaP resources. Indeed, in the two years since MicroMAS's launch, the maximum storage capacity of SD cards doubled from 256 GB to 512 GB. (Andrade, Press Releases, 2015) This trend (sometimes referred to as "Moore's Law") means that, almost inevitably, avionics designs will continue to improve as new versions of existing hardware are replaced.

6.3.2 Additional mission sets

MiRaTA and MicroMAS were able to be compared because of their similar mission sets. In order to apply this optimization approach to other mission sets, a greater number and variety of missions need to be analyzed.

6.3.3 Additional resources

In this thesis we only analyzed six resources: electrical power, volume, processing power, non-volatile memory, volatile memory, and radiation tolerance.[16] While certainly encompassing, this analysis was not exhaustive. Some additional resources for consideration in an expansion of our optimization approach include:

Quiescent Current – The current "leaked" to a component that it consumes when in a non-operational (quiescent) state. While generally on the order of micro amperes for small avionics components, when summed together, quiescent current can present a major drain on electrical power consumption.

---

[16] Thermal vacuum tolerance is also a key resource which we did not test due to time constraints

Single Event Effects – Our total ionizing dose radiation analysis was a simple before-and-after test of radiation exposure for damage to a system, rather than a real-time effect test. One of the major challenges presented by space radiation is its ability to alter electron flow to flip bits (1's become 0's and 0's become 1's) during normal spacecraft operations. This phenomenon is called a single event upset and a system's resistance to them could be considered an additional measure radiation tolerance.

Particle Radiation – The radiation tests we conducted were also conducted with a Cobalt-60 source, which produces only gamma rays. A more thorough analysis of radiation tolerance would also test avionics resistance to particle radiation such as alpha and beta particles.

Electrostatic Discharge (ESD) Resistance – Every electrical component is resistant to static discharge up to a certain voltage (anywhere from hundreds to thousands of volts). The minimum such resistance represents the susceptibility to damage in a non-ESD environment, as well as damage due to charge buildup on orbit. This resource could be calculated simply by looking through data sheets.

Thermal – All electrical components are also rated to a thermal survival and thermal operation range. These values represent the range of temperatures over which a component can survive in a dormant state without damage and operate with nominal characteristics respectively.

Vacuum – Electrical components are also rated to survive in vacuum conditions and operate for a set period of time. Functionality matching expected characteristics in a vacuum chamber would verify these ratings for the whole system.

Vibration – Launch into orbit presents a sometimes violent vibration environment for spacecraft which can damage or loosen avionics components. Especially with the increased popularity of surface mount technologies, vibration is a cause for concern that may limit the trade space for potential launch vehicles capable of supporting the vibration tolerances of avionics components.

Shock – Different that vibration, a shock test measures response to quick and violent impulses such as those experienced during various launch phases like stage separation.

6.3.4 Motherboard-specific optimization

There are sufficient resource characteristics and variability in designs of CubeSat motherboards that an optimization analysis of just that one avionics subsystem is possible. Additional motherboard-specific resources such as number of microcontroller pins, UART modules, SPI modules, I^{2}C modules, timers, comparators, as well as several of the resources we analyzed in thesis (processing power, volatile and non-volatile memory) already present more resources for analysis than the six we chose for this thesis.

6.3.5 MiRaTA hindsight

There are several things which, given the benefit of hindsight, we could have changed about MiRaTA's avionics design. First, we could have diverged further from Pumpkin's motherboard design and chosen a superior microcontroller to the PIC24FJ256GB210. For example, the PIC33EP512MU810 presents a nearly identical layout but with over twice as much program memory and half the RAM, which would allow for more of the spacecraft processes to be performed by the avionics microcontroller instead of distributing the processing to other systems (MiRaTA's design has a separate microcontroller for its payload). Beyond a simple improvement or modification in PIC selection, the selection of an ARM-based processor would enable even greater functionality at a minimal increase in SWaP resource consumption. The simplicity of programming an ARM processor over a PIC presents a tempting proposition for future avionics designs.

While not discussed in much detail in this thesis, monetary cost was higher than it could have been. The risk posture of a CubeSat program should allow for the use of circuit board manufacturers such as Osh Park which provide marginally lower quality PCBs for a fraction of the price of most manufacturers. Purchase of PCBs from these manufacturers, coupled with an in-house assembly process would increase the risk of flaws in either of those processes, but may very well remain within risk bounds set by the mission and would certainly save on cost (noting that the largest cost driver is staffing).

MiRaTA's primary radio also has presented a number of challenges inherent to a COTS system, such as difficulty of modification, troubleshooting without schematics, and dependence on vendors for firmware updates. Although certainly a daunting challenge to a university project, a 3 Mbps data rate is achievable. It is this author's hope that MIT's CubeSat program continues to develop in-house components for its spacecraft, including communications systems and ground station infrastructure.

Finally, it is my hope that the MIT Space Systems Lab and Lincoln Laboratory continue to collaborate on CubeSat missions in the future, building upon what has been learned in previous missions and establishing a robust, self-sufficient CubeSat program.

7 Works Cited

Andrade, J. (2014, September 11). *Press Releases.* Retrieved from SanDisk Web site: https://www.sandisk.com/about/media-center/press-releases/2014/sandisk-premieres-worlds-highest-capacity-sd-card-for-high-performance-video-and-photo-capture

Andrade, J. (2015, March 1). *Press Releases.* Retrieved from SanDisk Web site: https://www.sandisk.com/about/media-center/press-releases/2015/200gb-sandisk-ultra-microsdxc-uhs-i-card-premium-edition

Aniceto, R., Lohmeyer, W., & Cahoy, K. (2015). Total Ionizing Dose Requirements for Low Earth Orbit Small Satellites. *Journal of Small Satellites*, p. Pending Approval.

Ardizzoni, J. (2005). A practical guide to high-speed printed-circuit-board layout. *Analog Dialogue, 39*(3).

Atomic Energy of Canada Limited. (1968, July 6). Instruction Manual: Gammacell 220 Cobalt 60 Irradiation Unit. Ottawa, Canada.

Blackwell, W., Allan, G., Allen, G., Burianek, D., Busse, F., Elliott, D., . . . Byrne, J. (2014). *Microwave Radiometer Technology Acceleration Mission (MiRaTA): Advancing Weather Remote Sensing with Nanosatellites.*

Blackwell, W., Allen, G., Galbraith, C., Hancock, T., Leslie, R., Osaretin, I., & ... Erickson, N. (2012). Nanosatellites for earth environmental monitoring: the MicroMAS project. *Geoscience and Remote Sensing Symposium (IGARSS)* (pp. 206-209). Munich, Germany: IEEE International.

Blackwell, W., Allen, G., Galbraith, C., Leslie, R., Osaretin, I., Scarito, M., & ... Erickson, N. (2013). MicroMAS: A First Step Towards a Nanosatellite Constellation for Global Storm Observation. *27th Annual AIAA/USU Conference on Small Satellites*, (pp. SSC13-XI-1). Logan, Utah.

Colilli, S. (2011, February 28). *Operatori Irradiatori Gammacel e Cesio*. Retrieved from http://www.iss.infn.it/operatori

Elkman, W. R. (1983). Electrostatic charging and radiation shielding design philosophy fora synchronous satellite. *Journal of Spacecraft and Rockets, V*(20), 417-424.

Garber, S. (2007, October 10). *Sputnik and The Dawn of the Space Age*. Retrieved from NASA History: http://history.nasa.gov/sputnik/

Gell-Mann, M., & Lloyd, S. (1996, September/October). Information measures, effective complexity, and total information. *Complexity, 2*(1), 44-52. doi:10.1002/(SICI)1099-0526(199609/10)2:1<44::AID-CPLX10>3.0.CO;2-X

Kingsbury, R., Schmidt, F., Cahoy, K., Sklair, D., Blackwell, W., Osarentin, I., & Legge, R. (2013). TID Tolerance of Popular CubeSat Components. *Radiation Effects Data Workshop (REDW).* IEEE Nuclear and Space.

Krodel, J. (2001). *Commercial Off-The-Shelf (COTS) Avionics Software Study (No. AIR-130).* Washington, DC: FEDERAL AVIATION ADMINISTRATION WASHINGTON DC OFFICE OF AVIATION RESEARCH.

Lim, B., Shearn, M., Dawson, D., Parashare, C., Romero-Wolf, A., Russell, D., & Steinkraus, J. (2013, July). Development of the Radiometer Atmospheric CubeSat Experiment payload. *Geoscience and Remote Sensing Symposium (IGARSS)*, pp. 849-851.

Mairaj, A., & Tahir, R. (2014). *SWaP Reduction: Vital for Choice of Avionics Architecture.* Pakistan Aeronautical Complex, Avionics Production Factory. Kamra, Pakistan: International Conference on Engineering and Emerging Technologies.

Manyak, G., & Bellardo, J. (2011). PolySat's Next Generation Avionics Design. *Space Mission Challenges for Information Technology (SMC-IT)* (pp. 69-76). Washington, DC: IEEE Fourth International Conference.

Marlow, W., Marinan, A., Riesing, K., Nguyen, T., Cahoy, K., Byrne, J., . . . Thompson, E. (2015). *Attitude Determination and Control Approach to Achieve Co-Located Microwave Radiometer and GPS Radio Occultation Measurements on a Nanosatellite.* AAS.

McCormick, R. (2014, September 12). *SanDisk's 512GB SD card is teh biggest in the world.* Retrieved from The Verge: http://www.theverge.com/2014/9/12/6139057/sandisks-512gb-sd-card-is-the-biggest-in-the-world

Nathanson, H. C. (2006). *United States Patent No. 7102472.*

Neil, J. (2009). *Simple Complexity: A Clear Guide to Complexity Theory.* London, UK: Oneworld Publications.

Obland, M., Klumpar, D., Kirn, S., Hunyadi, G., Jepsen, S., & Larsen, B. (2002). Power subsystem design for the Montana EaRth Orbiting Pico-Explorer (MEROPE) CubeSat-class satellite. *Aerospace Conference Proceedings, 2002. 1*, pp. 1-465. Big Sky, Montana: IEEE.

Planet Labs Inc. (2015). *About.* Retrieved from Planet Labs Web sit: https://www.planet.com/about/

Pumpkin Inc. (2003). *The Genesis of the CubeSat Kit*. Retrieved from CubeSat Kit Web Site: http://www.cubesatkit.com/content/history.html

Rissanen, J. (1989). *Stochastic Complexity in Statistical Inquiry.* Singapore: World Scientific.

ScienCentral, Inc and the American Institute of Physics. (1999). *Integrated Circuits*. Retrieved from Public Broadcasting Service Web site: http://www.pbs.org/transistor/background1/events/icinv.html

Sidwar, K. (2015, January 22). *A Web Developer's Guide to Communication Protocols (SPI, I2C, UART, GPIO).* Retrieved from Tessel: https://tessel.io/blog/108840925797/a-web-developers-guide-to-communication-protocols

Sinclair, D., Enright, J., Dzamba, T., & Sears, T. (2015). Custom Optics vs Modified COTS for Small Spacecraft. *Small Satellite Conference Proceedings.* Logan, Utah.

Sinclair, I. J. (1995). *The use of commercial off-the-shelf (COTS) software in safety-related applications.* London, UK: Sudbury: HSE Books.

Springmann, J. C., Kempke, B. P., Cutler, J. W., & Bahcivan, H. (2012). Development and Initial Operations of the RAX-2 Cubesat. *ESA/CNES Small Satellites Systems and Services Symposium.*

The Tauri Group. (2015). *State of the Satellite Industry Report.* Alexandria, VA: Satellite Industry Association. Retrieved September 9, 2015, from http://www.sia.org/wp-content/uploads/2015/06/Mktg15-SSIR-2015-FINAL-Compressed.pdf

Verle, M. (2008). *PIC Microcontrollers.* Belgrade, Serbia: MikroElektronika.

Verle, M. (2010). *PIC Microcontrollers - Programming in Basic.* Belgrade, Serbia: mikroElektronika; 1st edition.

Wang, G., Wang, C., Zhou, B., & Zhai, Z. (2009). Immunevonics: Avionics fault tolerance inspired by the biology system. *Computational Intelligence and Industrial Applications. 1*, pp. 123-126. Xi"an: PACIIA 2009. Asia-Pacific Conference.

Watkins, C. B., & Walter, R. (2007). Transitioning from federated avionics architectures to integrated modular avionics. *Digital Avionics Systems Conference, 2007* (pp. 2-A). Dallas, TX: IEEE/AIAA 26th.

Weaver, R. L., Sanders, B., Gasiewski, A. J., Periasamy, L., Gallaher, D. W., & Scambos, T. A. (2012, December). PolarCube-A CubeSat to Monitor the Sea Ice and Atmosphere Temperature Structures. *AGU Fall Meeting Abstracts*, pp. (Vol. 1, p. 08).

Wilcock, G., Totten, T., Gleave, A., & Wilson, R. (2001). The application of COTS technology in future modular avionic systems. *Electronics & communication engineering journal, 13*(4), 183-192.

Wu, D., Esper, J., Ehsan, N., Johnson, T., Mast, W., Piepmeier, J. R., & Racette, P. E. (2015). IceCube: CubeSat 883-GHz Radiometry for Future Ice Cloud Remote Sensing.